Mapping of γ -emitting radionuclides from Princess Mine Dump and the potential radiological effects on human beings

M. M. Magagula

Mini-dissertation submitted in partial fulfilment of the requirements for the degree Master of Science in Applied Radiation Science and Technology at the Mafikeng Campus of the North-West University

Supervisor: Prof M.V. Tshivhase

Co-Supervisor: Prof M.M. Mathuthu

May 2015

Declaration

I, the undersigned, declare that the following document reports an original research project carried out at the Centre for Applied Radiation Science and Technology at the North-West University, Mafikeng campus in collaboration with the Council for Geoscience. This work has not been submitted in part or whole for any degree at any university before. The data presented is original and all analysis was done by the author under the guidance of the supervisor, any other sources of data acquired through collaborative work have been fully acknowledged.

Magagula M. M. .....

Date 07/10/2015

Dedication

This work is dedicated to the late Duma Methula. He was a brother, a friend and a true confidant in good and in tough times. He has been the main source of inspiration throughout, and may his rest in peace.

Acknowledgements

Special thanks are forwarded to the following:

- Council for Geoscience for funding of the project,
- CARST for the opportunity to perform the project,
- Animal Health and Chemistry departments from the North-West University for providing access to their facilities, expertise and equipment,
- Prof A Fanhoof for his scientific guidance throughout the project,
- Colleagues, classmates and research partners, Sibusiso Dlamini and Thulani Dlamini for their encouragement, and
- My supervisors Prof M. V. Tshivhase and Prof M. M. Mathuthu for their undivided attention to the project.

Abstract

The study was carried out at the Princess dump, an old abandoned mine tailing storage facility in the Witwatersrand region of South Africa. It was aimed at identifying the NORMS in the dump and their activity concentrations using a High Purity Germanium detector. According to literature the South African gold mines are associated with high levels of uranium. The mining activities in general tend to elevate the concentrations of NORMS near the earth surface. The main objectives were to identify the available NORMS from the tailing, measure their activity concentrations and using hazard indices and dose calculation to estimate the risk the mine dump poses to the communities around it. The radionuclides were identified and their average activity concentrations were 162.8 ± 32 Bq/kg, 24. 9 ± 1.3 Bq/kg, 214.5 ± 37 Bq/kg, and 97.4 ± 8.5 Bq/kg for ^{238}U, ^{232}Th, ^{226}Ra, and ^{40}K, respectively. The activity concentrations were compared to the world average concentrations determined by UNSCEAR, 2008 of 33 Bq/kg, 35 Bq/kg, 45 Bq/kg and 412 Bq/kg for ^{238}U, ^{226}Ra, ^{232}Th and ^{40}K, respectively. The average activity concentration of ^{226}Ra was found to be the only one which is higher than the UNSCEAR values while the rest were only below. The average radium equivalent of 233 Bq/kg and the absorbed dose at 1m above the dump of 94.6 nGy/h was determined. The hazard index of 0.68 was calculated from the data and was found to comply with the UNSCEAR limits, since it is below one. The results indicate that Princess Mine Dump does not pose any radiological hazard to the nearby community by its presence. The average activity concentrations are slightly lower than the world averages according to UNSCEAR values. It is recommended that the detailed dust transfer measurements be undertaken in the vicinity of the communities so as ensure that final recommendation can be drawn to assure the safety of the public living in the nearby communities.

List of tables

Table 2.1: Radiation weighting factors for different radiation 28

Table 2.2: Tissue weighting factors 30

Table 4.1: Activity Concentration for the NORMs and their progenies Bq/kg for the soil taken with at 15cm below ground level 43

Table 4.2: Activity Concentration for the NORMs and their progenies in Bq/kg for the soil taken with 100 cm below ground level 45

Table 4.3: Average activity concentrations for the radionuclides in the topsoil, bottom soil and the whole mine dump 47

Table 4.4: The calculated activity concentrations from dust concentration of 50μg/cm^3 52

Table4.5: The Annual effective dose equivalent for different age groups 53

Table 5.1: Gamma dose rates in nGy/h and annual effective dose rates in mSv/yr from selected mining areas around the world 58

List of figures

Figure 2.1: Transmission curve for alpha particles mono energetic electrons (betas) and gamma rays with their respective mean ranges 9

Figure 2.2: A schematic diagram for photo electric emission 10

Figure 2.3: A schematic diagram of Compton scattering 11

Figure 2.4: A schematic diagram of pair production 12

Figure 2.5: Two gamma detectors and the gamma spectroscopy set up 14

Figure 2.6: Decay series for Thorium and Uranium 17

Figure 2.7: A side view of Princess Mine Dump 20

Figure 2.8: An aerial view of Princess Mine Dump and its surrounding areas 21

Figure 2.9: secular equilibrium 23

Figure 2.10: Transient equilibrium 24

Figure 2.11: A schematic set-up for ICP-MS spectrometer 33

Figure 3.1: An aerial view of Princess Mine Dump showing also the different sampling points 35

Figure 3.2: A manual auger for extraction of soil samples 36

Figure 3.3: The energy calibration curve 38

Figure 3.4: efficiency calibration of the GCD-96 high purity germanium detector 40

Figure 4.1: a typical gamma spectrum for a soil sample taken from Princess Mine Dump 42

Figure 4.2: activity concentrations in Bq/kg for each sampling point from Princess mine dump 46

Figure 4.3: ratios of top to bottom soil for the different radionuclides 48

Figure 4.4: dose rate against each sampling point 49

Figure 4.5: The radium equivalent against each sampling point 50

Figure 5.1: Average activity concentration in Bq/kg for Princess Mine Dump and two other places and also the UNSCEAR world average 54

Figure 5.2: A comparison between the annual effective dose from Princess Mine Dump with two other places 57

List of abbreviations

UNSCEAR – United Nations scientific committee on the effects of atomic radiation

TENORM - Technologically Enhanced Naturally Occurring Radioactive Material.

NORM – Naturally Occurring Radioactive Material

ICRP - International Commission on Radiological Protection

CARST- Centre for Applied Radiation Science and Technology

NNR- National Nuclear Regulator

ICP-MS – inductively coupled plasma mass spectrometry

HPGe – high purity germanium detector

H_{EX} – hazard index

PPIC - Parallel Plate Ionization Chambers

IAEA - International Atomic Energy Agency

AEDE - Annual Effective Dose Equivalent

OGP – Oil and Gas Production

TSF – Tailing Storage Facilities

RBE – relative biological effectiveness

Table of Contents

Declaration ii

Dedication iii

Acknowledgements iv

Abstract v

List of tables vi

List of figures vii

List of abbreviations ix

CHAPTER 1: INTRODUCTION AND PROBLEM STATEMENT 1

1.1 Introduction 1

1.2 Problem statement 3

1.3 Justification and significance of the study 4

1.4 Aim and objectives 4

1.4.1 Aim 4

1.4.2 Objectives 4

CHAPTER 2: LITERATURE REVIEW 6

2.1 Introduction 6

2.2 Radioactivity 6

2.3 Types of radioactive decay 7

2.3.1 Alpha decay 7

2.3.2 Beta decays 8

2.3.3 Gamma decays 9

2.4 Interaction of gamma energy with matter 9

2.4.1 Photo electric effect 10

2.4.2 Compton scattering 12

2.4.3 Pair production 13

2.5 Gamma Spectroscopy 13

2.6 Scintillation Detectors 15

2.7 Semiconductor Detectors 16

2.8 Gas ionisation detectors 16

2.9 Naturally Occurring Radioactive Materials (NORMs) 17

2.9.1 NORMs in mining 18

2.9.2 Tenorms 20
2.10 Princess Mine Dump 21
2.11 Radiation equilibrium 22
2.11.1 Secular equilibrium 23
2.11.2 Transient equilibrium 24
2.12 Mobility of NORMs in sediments 25
2.13 Biological effects of radiation 27
2.13.1 Radiation dosimetry 27
2.13.2 Risk assessment 31
2.14 Inductively Coupled Plasma Mass Spectroscopy (ICP-MS) 33
CHAPTER 3: METHODOLOGY 35
3.1 Introduction 35
3.2 Sample collection 35
3.3 Sample Preparation 37
3.4 Calibration of the instrument 38
3.4.1 Energy calibration for gamma spectroscopy 38
3.4.2 Efficiency calibration for gamma spectroscopy 39
3.4.3 Calibration of the ICP-MS 41
3.5 Data Acquisition 42
CHAPTER 4: RESULTS AND DISCUSSION 43
4.1 Introduction 43
4.2 Results 43
4.2.1 Determination of radioactivity 44
4.3 Investigation of mobility of radionuclides 48
4.4 Determination of radium equivalent and absorbed dose 49
4.5 Estimation of transfer to dust and calculation of AEDE 51
4.5 Discussion 54
CHAPTER 5: CONCLUSIONS AND FUTURE WORK 60
5.1 Conclusions 60
5.2 Future work 61
REFERENCES 62
Appendices 69

CHAPTER 1: INTRODUCTION AND PROBLEM STATEMENT

1.1 Introduction

Since its discovery early in the 19th century, by Marie Curie and Henry Becquerel, radioactivity has become a major part of the human life. Radioactivity has had both useful applications and consequences in our everyday activities (Sroor et al, 2001), ranging from the medical applications to the military usage by most governments. In the turn of the 20th century, a larger part of radioactivity became a major cause for concern; this is the naturally occurring radioactive materials. These naturally occurring radioactive materials, are found everywhere on the earth's surface (Ballare et al, 2000). They are in manageable concentrations unless tampered with by man-made practices. Mining has been one of the major landscape and environmental polluters (Robins, 2004). Part of the environmental pollution comes in the form of deposition of higher level naturally occurring radioactive material.

Over the years mining has been the major source of income for many governments and the government of South Africa is one of the major beneficiaries of mining (Yager, 2007). According to Dr A Turton, the major economic boost that has been brought about by the mining industry has come at a very costly price (Irin humanitarian news, 2008). In an interview, he explicitly said that South Africa is paying the price of gold. This is mainly because of the fact that, some mining areas in the country, particularly the Witwatersrand region have been very productive in gold extraction yet with the most elevated NORMs concentration. During mining, the unwanted waste is deposited in piles which are called tailing storage facilities (Irin humanitarian news, 2008). These tailing storage facilities have in previous cases been found to have elevated radiation levels.

The Princess Mine Dump is one of those tailing storage facilities, found in Roodepoort in the Gauteng province of South Africa. It is surrounded by residential settlements of Davidsonville and a manmade wetland in close proximity as shown in Figure 2.8 (Ngigi, 2009). The abandoned mine tailing has not been rehabilitated and is currently impacting on the surrounding environment (Speelman et al, 2005). The water streams in the area have been reported to be of very poor quality, with low pH values and very high conductivity (Winde, 2010). Some studies claim that this is

caused by leaching of nuclides from mine tailings (Winde, 2010). The area also experiences high wind that blows through the region and especially just before the spring rains (Smith, 1997). This makes it a good area to perform a radioactivity survey especially on the dust particles in the nearby community.

This study therefore aims to establish the amount of radionuclides in the mine tailing (Princess Mine Dump) and map them accordingly with their respective activities and also find out how much of those radionuclides are carried by the dust to the nearby community. The first chapter includes the problem statement, objectives and the justification of the study. The second chapter looks at the literature review. The third chapter is the methodology which outlines and explains the methods that are used in the whole study. Chapter four reports the results and the analysis of the results, and discussion. Chapter five is for the conclusion and possible future work related to the same study.

1.2 Problem statement

Radiological environmental issues associated with the major contributor to the economy of the country, gold mining, have to be fully understood and managed. Due to the mining of heavy metals like gold, many radioactive materials find their way into the land that is in contact with the people and the environment. For proper regulation and also rehabilitation a well-informed database of the amount of radionuclide concentration on the previous mining areas is needed.

In a study that was done in Nigeria on a mine tailing, Dutse-Maru, in the Jos region, it was found that the activities of Thorium-232 and Radium-226 were higher than the values that are allowed by UNSCEAR. In Princess Mine Dump, high dose rates were also discovered. It is believed that the gold mine tailings are the ones responsible for the radioactive pollution in the Witwatersrand region of South Africa.

Princess Mine Dump is a storage facility for an old gold mine, and it is known that gold mining especially in South Africa is associated with the presence of Uranium. This then presents the possibility of the dump being contaminated with radionuclides. According to, the NNR annual status report, 2006, the Gauteng region has many tailing storage facilities from old gold mine and the water sources from areas with these mine tailings have shown high concentrations of radionuclides.

In the light of these observations, it is reasonable to assume that an old mine tailing facility, like Princess Mine Dump, would have a huge possibility of being radioactive. Therefore this study was to identify and map the gamma-emitting radionuclides from Princess Mine Dump, analyse the activity concentrations of those available radionuclides and calculate the dose rates to the public.

1.3 Justification and significance of the study

As it has been highlighted in the sections above, the study is a radio analytical survey of an old Gold mine tailing facility called Princess Mine Dump. This is expected to yield data that can be used as a database for the mine tailing facilities. It is expected to shed light on the curious parties which are the media and population near the tailing of the composition of the tailing facility. The analysis of the findings is expected to estimate the potential health hazards that are posed by the presence of the mine dump to the people living near it. Lastly, looking at how close the nearest community is, to the mine tailing, a detailed study of the radioactivity of the dump seems necessary.

1.4 Aim and objectives

1.4.1 Aim

The focus of the study is to investigate the health risk that is posed to the people living near Princess Mine Dump, spending time on top of the Dump and also the environmental effects to the surroundings. This study therefore aims mainly at identifying the radionuclides that are present in the dump, analysing their activity concentrations and the potential radiological hazard to the community and the environment around Princess Mine Dump. The estimated transfer of radionuclides to dust will be determined.

1.4.2 Objectives

The objectives of the study are:

- To identify the different radionuclides that are present at the mine dump, using high purity Germanium detector (HPGe);
- To analyse the concentrations of the different radionuclides at the dump, using both the HPGe and ICP-MS;
- To calculate the concentrations of the parent nuclide from the activities of the daughters, this can be determined using secular equilibrium.
- To determine the mobility of the radionuclides with depth;
- To calculate the estimated internal exposure from inhaled dust from the mine tailing;

- To determine the annual effective dose equivalent to the public and the hazard index (H_{ex}) and compare with those given by international regulatory bodies.

CHAPTER 2: LITERATURE REVIEW

2.1 Introduction

This chapter reviews the different concepts that affect the experimental procedure as well as the theory needed in order to conduct the experiments. Involved also are the different equations that are important for the analysis of the data obtained and the principle of operation of the instruments that were used as well as the background information on other similar studies that have been conducted elsewhere.

2.2 Radioactivity

Radioactivity refers to the emission of radiation by a nucleus of an atom due to instability. Instability in this case, is the imbalance between the nucleons (i.e. the neutrons and the protons), and also the amount of energy that a certain element has (Krane, 1998). According to elementary atomic physics, the nucleons of a nuclide follow a certain distribution in order for it to be stable. When a nuclide is unstable it undergoes radioactive decay and it will emit radiation in the form of particles or energy. The particles can be alpha (α) particles, beta (β) particles, neutrons, etc. (Ozawa, 2004). The energy is usually gamma (γ) rays or sometimes X-rays. An atom or nuclide undergoing this kind of emission is said to be radioactive. An important measurement parameter of radioactivity is the half-life ($T_{1/2}$), which is defined as the time it takes for a particular nuclide to decay to half of its original amount (John et al, 2009). Most radioactive nuclides are either manmade or natural and cosmogenic and the manmade are a consequence of human practices. These include nuclear power reactors, nuclear accidents e.g. Fukushima, 2011, and the bombs that were dropped in Japan many decades ago (Smith and Baxter, 2007). Radiation is measured using a quantity called Activity, with its units being, disintegration per second or Becquerel (Bq). The formula for activity is shown in equation (1).

$$A = \lambda N \qquad (1)$$

Where A - is the activity of the sample,

N - is the number of nuclei in the sample and,

λ - is the decay constant of the nuclide which is derived from its half-life as shown in equation (2).

$$\lambda = ln2/T_{1/2}, \quad (2)$$

Where $T_{1/2}$ - is the half-life of the nuclide

Nuclear decay can be best described using the decay equation, equation (3):

$$N(t) = N_0 exp(-\lambda t), \quad (3)$$

Where N_o – is the initial number of nuclei in the sample

t - is the time taken

When equation (1), is substituted into equation (3) it yields equation (4), which can be used to estimate the activity ($A(t)$) of a certain nuclide at time t, if the initial activity (A_0) is known. This can be used also to estimate the initial activity if the final activity is known by simply transposing the formulae.

$$A(t) = A_0 e^{-\lambda t} \quad (4)$$

2.3 Types of radioactive decay

2.3.1 Alpha decay

Alpha particles are made up of two protons and two neutrons, often identified as the helium nuclei. Most heavy radioactive nuclides (i.e. nuclei with Z > 82) often undergo alpha decay and emit alpha particles. During this process the nuclide emerges with a proton number that is reduced by two and a mass number that is reduced by four. The nuclear equation, (5) shows alpha decay.

$$^{A}_{Z}X_N \rightarrow ^{A-4}_{A-2}Y_{N-2} + \alpha \quad (5)$$

Where : A is the mass number
z –atomic number
N –neutron number
$^{A}_{Z}X_N$–is the parent nuclide
$^{A-4}_{A-2}Y_{N-2}$- is the daughter nuclide or the nuclide after undergoing alpha decay
α- is an the alpha particle

The theory of alpha emission was developed by Gamow, Gurney and Cordon. They assumed the parent nucleus to be containing a separate alpha particle trapped by a certain amount of energy barrier, or the nucleus to exist as different alpha particles that exist separately in the nucleus but held together by a certain amount of energy

(Krane, 1988). This energy acts as a barrier that the alpha particle has to overcome in order to escape. Poenari et al described alpha decay as a fission-like process, where fission is the splitting of atomic nuclei into different fragments. This theory can further be explained better by the tunnelling theory (Poenari et al, 1979). Tunnelling can be explained by quantum mechanics. This study only seeks to state the existence of alpha decay and describe alpha particles and the energy changes involved.

Alpha particles compared to other radiation particles has a larger mass and charge, hence it causes a lot of ionisation after emission. They travel short distances because they deposit a lot of energy along the way (Harvey, 1969).

2.3.2 Beta decays

Beta particles are electron-like particles that originate from the either proton-rich or neutron rich unstable nuclei. The particle has an electronic charge and its mass is similar to that of an electron. The process of beta emission occurs with the change of the proton number Z either increasing by one or the decreasing by one, while the mass number or the atomic mass stays the same, and then a beta particle is emitted. This process can also happen through electron capture where by the nucleus capture a k- orbital electron. The beta electron can either have a positive or a negative charge depending on the process through which it was emitted (Harvey, 1969). The three different processes can be better described by the three nuclear equations.

$$n \rightarrow p^{+} + \beta^{-} + \bar{\upsilon} \qquad \text{(Beta minus emission)} \qquad (6)$$

$$p^{+} \rightarrow n + \beta^{+} + \nu \qquad \text{(Positron emission)} \qquad (7)$$

$$p^{+} + e^{-} \rightarrow n + \nu \qquad \text{(Electron capture)} \qquad (8)$$

Where n is a neutron

P - is a proton

E - is an electron

β - is a beta particle

ν - is an antineutrino

$\bar{\upsilon}$ - is a neutrino

The positively charged beta particle is called a positron. According to the *Pauli* neutrino hypothesis, beta emission is followed by a second particle called the neutrino which follows positron emission and electron capture and the antineutrino follows the electron emission which is the negative beta particle emission.

Beta particles are more penetrative than alpha particles in nature. This property is hugely owed to the lightweight, and smaller charge compared to alpha particles. They travel longer distances than alpha particles and cause less ionisation (Krane, 1988).

2.3.3 Gamma decays

Gamma radiation is charge-less and mass-less electromagnetic energy. It is similar to visible light and X-rays in terms of properties. The only distinguishing factor from other electromagnetic radiation, is the wavelength hence the frequency. Gamma emission is usually released by unstable nuclei in order to remove the excess energy to obtain stability. This emission usually follows alpha or beta decay. This is because the two types of decay usually leave the nuclide unstable after the emission of either a gamma or a beta particle (Krane, 1988).

Gamma rays are the most penetrative and deposit very small amounts of energy in their path as compared to alpha and beta particles. Being charge less makes them even less ionising hence they travel very long distances after emission and they ionise indirectly (Krane, 1998).

2.4 Interaction of gamma energy with matter

With reference to the fact that gamma rays are uncharged particles, unlike alpha and beta particles, they travel longer distance in matter and have much greater penetrating power, than the two. Figure 2.1 shows the different ranges covered by the three types of radiation. It can be seen that gamma rays cover a much greater range than alpha and beta particles. The significant characteristic of gamma rays is that their absorption is an exponential decay function.

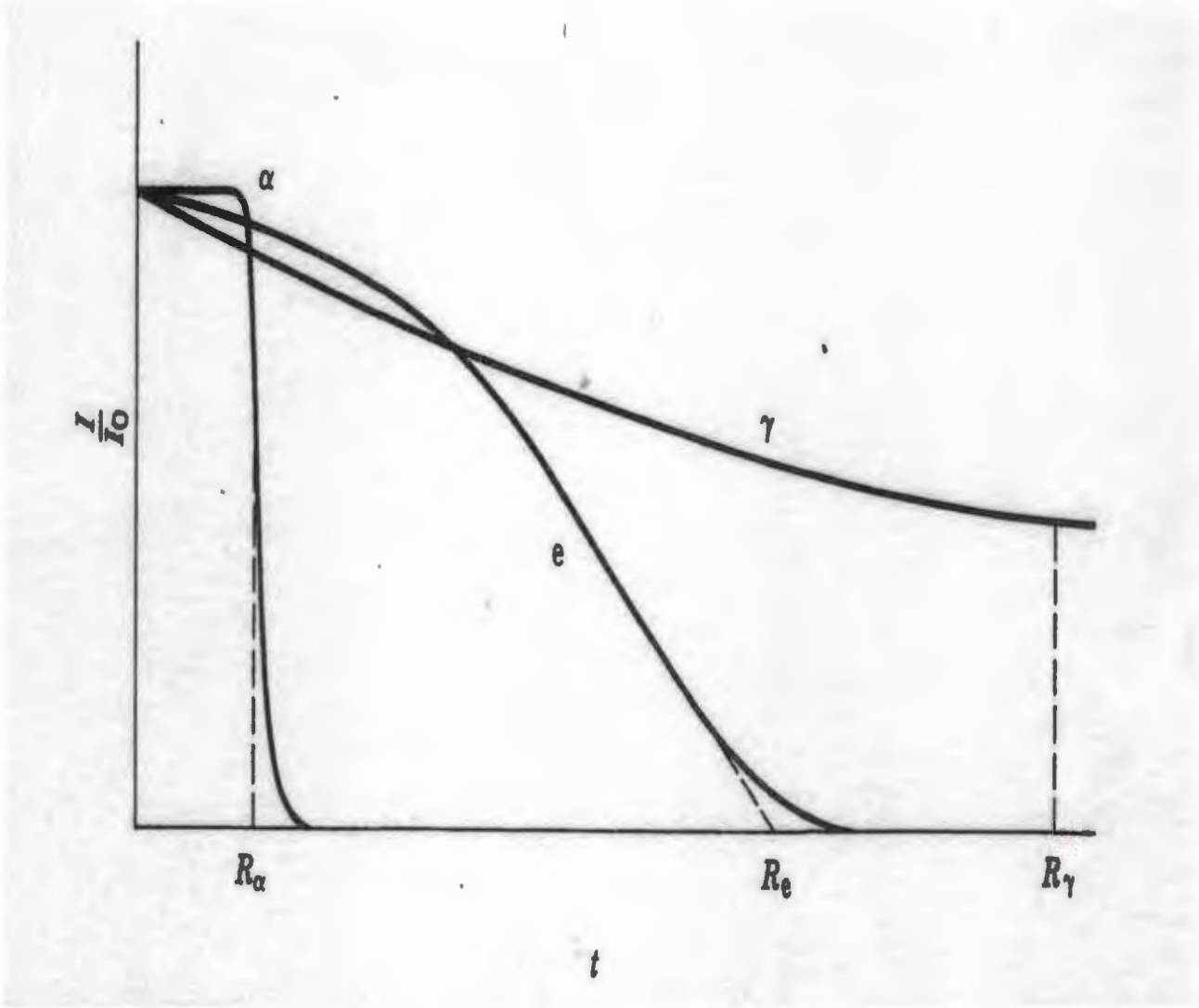

Figure 2.1: The transmission curve for alpha particles, mono energetic electrons (beta particles) and gamma rays with their respective mean ranges (Santawamaitre, 2012)

Gamma rays in general interact with matter in three different ways, which are namely the photo electric effect, Compton scattering and pair production.

2.4.1 Photo electric effect

This is the process whereby electrons are ejected from a surface through the action of electromagnetic radiation. This effector process was discovered by Heinrich hertz in 1887 and explained by Albert Einstein based on the quantum concepts of Max Plank. Electron emission occurs only if the frequency of incident light exceeds the characteristic cut off frequency of the particular surface. When the energy photon interacts with the absorber material, a photo electron is ejected with a kinetic energy

that is given by the incident photon energy ($h\nu$) minus the binding energy of the electron as shown in equation (9). A schematic diagram of the photo electric effect is shown if figure 2.2 below. (Hobbie and Roth, 2007)

$$KE = h\nu - E_B \quad (9)$$

Where KE – is the kinetic energy

h – is planks constant

ν – is the frequency

E_B – is the binding energy of the electron

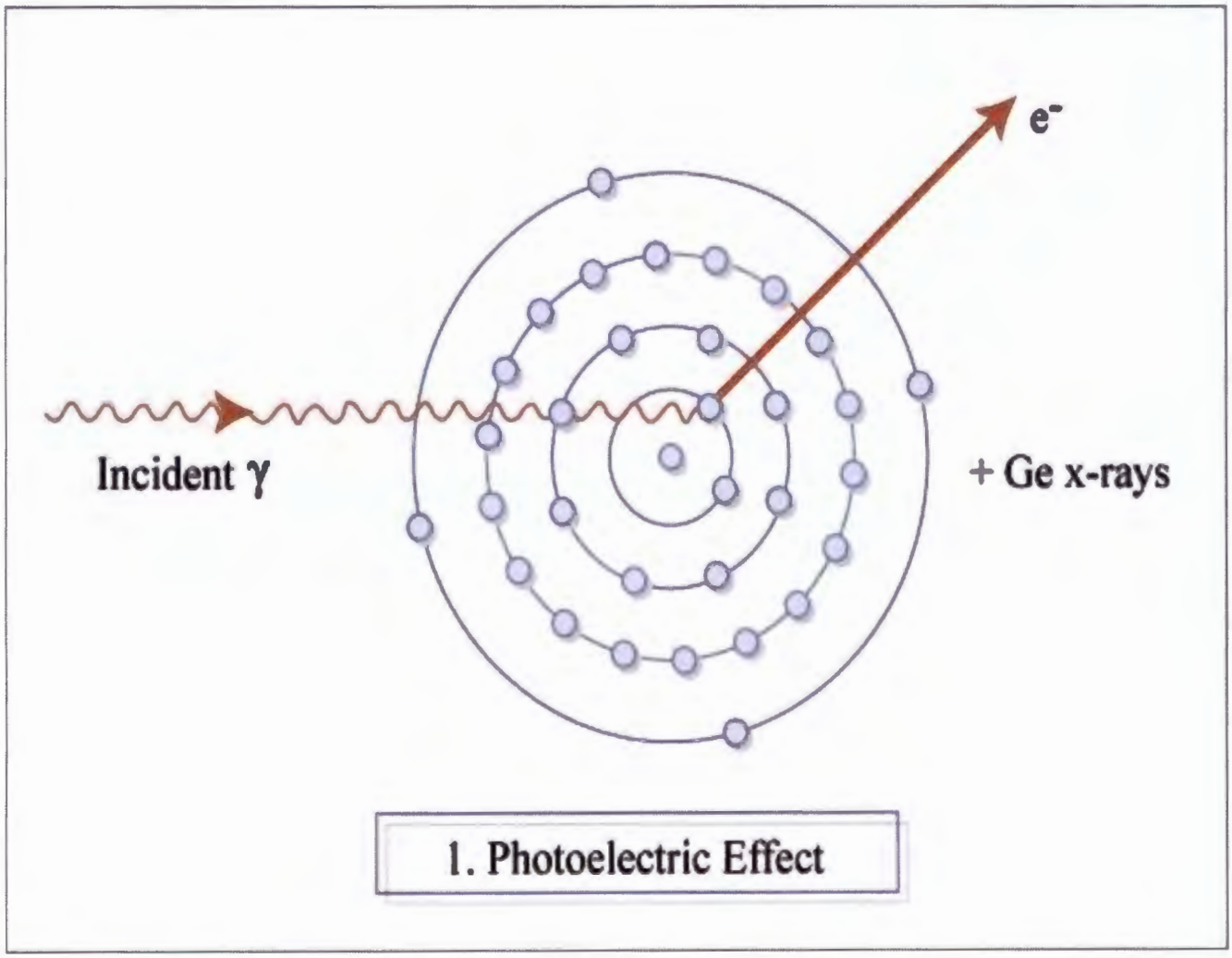

Figure 2.2: Schematic diagrams for photo electric emission (Santawamaitre, 2012)

2.4.2 Compton scattering

Compton scattering, also known as incoherent scattering is when the incident photon interacts with electrons of atoms in matter. Here the photon scatters on the atomic electrons hence losing some of its energy also can knock off an electron in the process hence ionising the atom in question (Krane, 1998). Figure 2.3 shows a schematic diagram of a Compton scattering event.

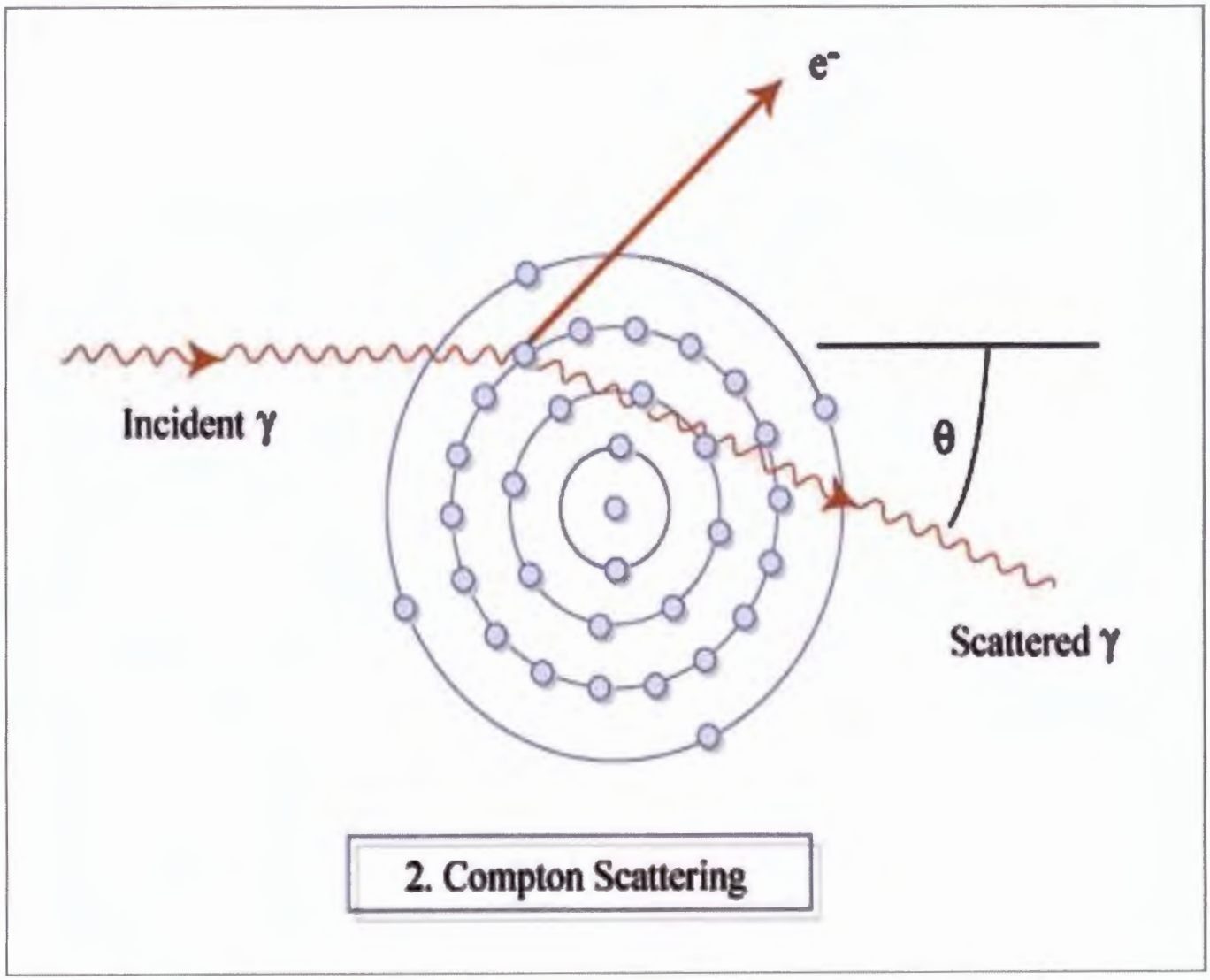

Figure 2.3: A schematic diagram of Compton scattering (Santawamaitre, 2012)

The result of Compton scattering is that the incident gamma ray loses energy and deflects from its original direction. Also an electron is ejected called a recoil electron. During the process linear energy and momentum are conserved and are related also to the angles at which they are deflected.

2.4.3 Pair production

Pair production usually happens when a gamma photon has energy that is almost equal or comparable to twice the rest mass of an electron which is about 1.02 MeV. The photon therefore splits into two particles which are the electron and the positron. These are charged hence they can cause direct ionisation to matter (Krane, 1998). This interaction takes place within the coulomb field. When the photon is absorbed into the vacuum, it is converted into an electron and positron pair shown in figure 2.4.

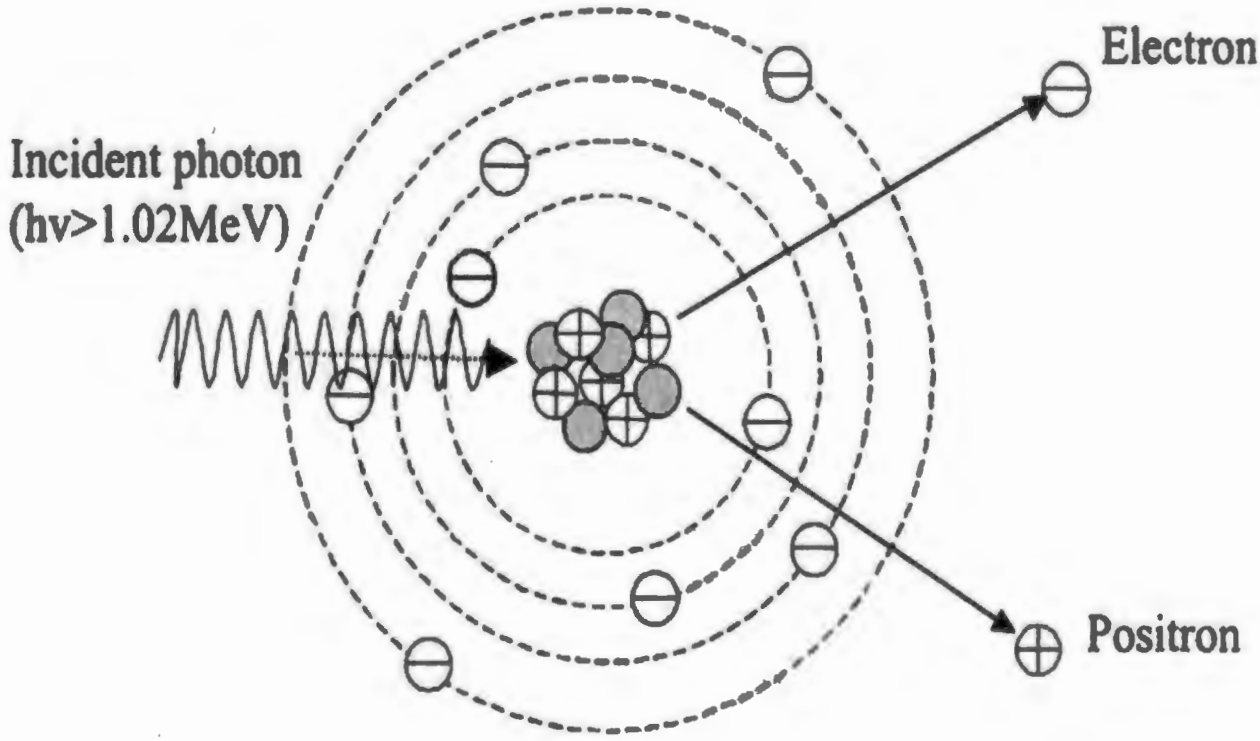

Figure 2.4: A schematic diagram of pair production (Srivastava, 2006)

2.5 Gamma Spectroscopy

Gamma spectroscopy is a quantitative study of energy spectra and gamma ray sources in a laboratory. It exploits gamma radioactivity. In gamma spectroscopy gamma radiation is picked up by detectors, which differentiate between the gamma

rays using their difference in energy (Lutz, 2001). Knowing the different gamma energies for different gamma emitters enables the detection of gamma emitting radionuclides in any material. A detector is used to detect different gamma energies, which can help to identify the different nuclides they represent. A library, like the one shown in annexures 1 a) to c) is used to match each gamma ray with a radionuclide. There are a number of detectors of gamma rays, all working on almost the same principle (Bode, 1998). They use the interaction of gamma radiation with matter. Gamma radiation interacts with matter in three different ways namely, Compton scattering, photoelectric effect and pair production (Krane, 1998) (see 2.4.1 to 2.4.3). However of more importance are the types of gamma spectroscopy detectors, which are also divided into three. They allow the gamma rays to enter the detector and interact with the atoms of the detector active site, in the process releasing part or all the energy to the atom. This interaction releases a relatively large amount of low energy electrons, which are collected as a voltage pulse, for analysis by electric circuitry (Krane, 1998). The electronics amplify and count the number of similar gamma energy pulses, and which are reported in the form of counts per second. From the number of counts and the time taken to read those counts the activity of samples can be calculated using equation (10).

$$Activity(Bq) = \frac{CPS}{B.I \times Eff} \pm \frac{CPS_{error}}{B.I \times Eff} \qquad (10)$$

Where CPS - is counts per second

B.I - is the branching intensity

Eff - is the efficiency of the detector

The branching intensity arises from the fact that gamma emitters emit gamma photons of different energies. These different energies are called branches and their statistic percentages are found in annexure 1. There are three types of gamma detectors, namely: the gas ionization chamber detectors, scintillation detectors and the semiconductor detectors (Lutz, 2001). Figure 2.5 shows two separate images; the first one is two gamma detectors, a portable GCD germanium detector and a larger high purity germanium detector. The second picture in the figure shows a setup for a gamma spectrometer, inside the lead shield and a computer for controlling the detector and data acquisition.

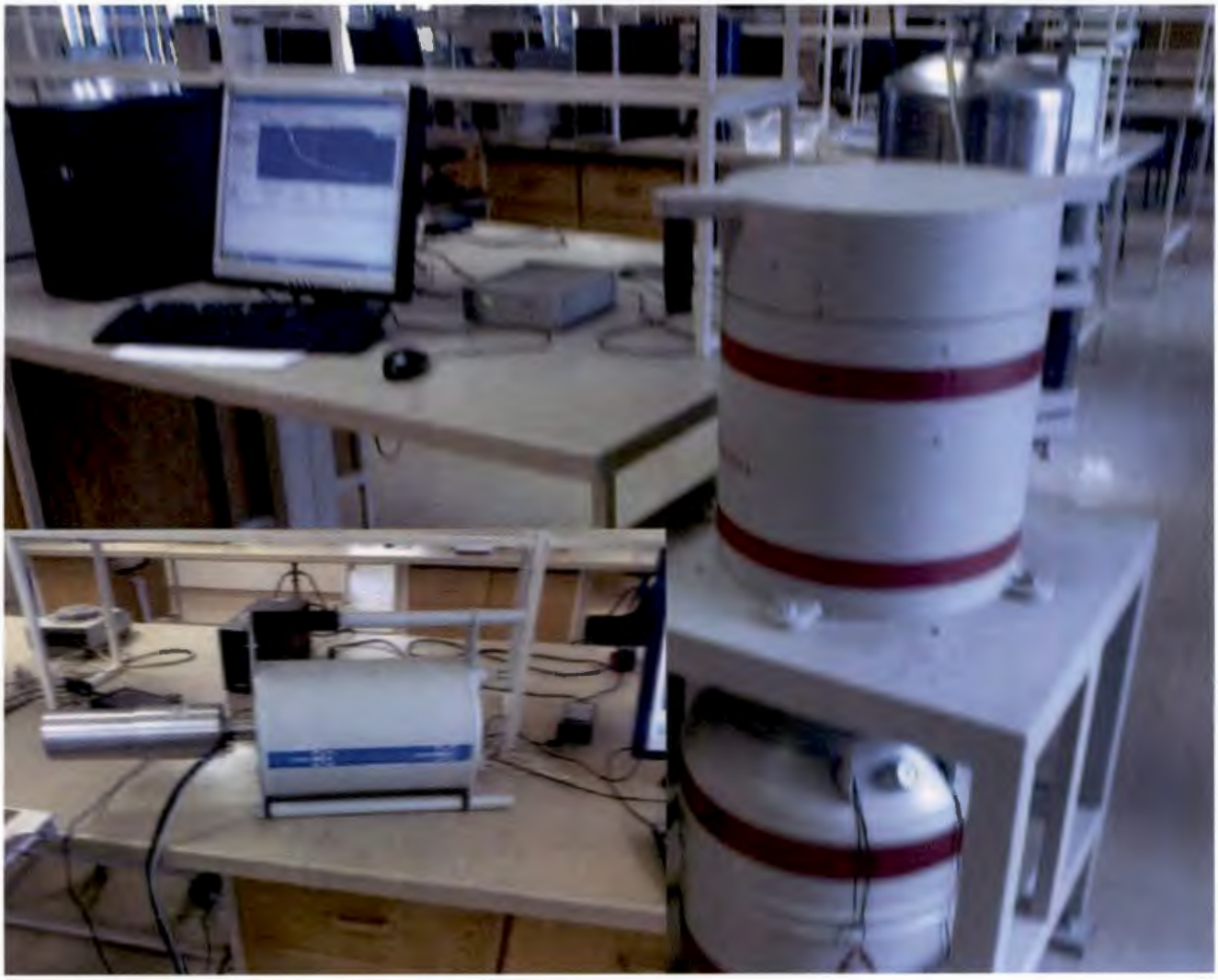

Figure 2.5: Two gamma detectors and the gamma spectroscopy set up

2.6 Scintillation Detectors

Scintillators fluoresce when they are hit by ionising radiation. This means that they produce a flash of light which is amplified by photomultiplier tubes. Scintillators can be organic or inorganic. Organic scintillators are solid crystals, plastics, synthetic polymers, etc. and inorganic scintillators include bismuth permanganate, sodium iodide doped with thulium, caesium doped with sodium. The most common is the sodium iodide detector (Bode, 1998). Although scintillation detectors are known for their high efficiency in acquisition but they have a very low or poor resolution, hence for this study they are not used.

2.7 Semiconductor Detectors

Semiconductor detectors use semiconductor material for the detection of radiation. Semiconductor material has a completely filled valence band and an empty conduction band. In most cases semiconductors are usually doped with impurities to lower their energy gap, but some are not (Yu and Cardona, 2010). The energy from the radiation comes into contact with the semiconductor crystal and it changes it into a conductor by lifting the electrons to the conduction band. This makes an electric pulse which is picked up and analysed by electric circuitry (Bode, 1998)

For very sensitive crystals, the semiconductor may have enough energy to be a conductor even at room temperature and this may affect the measurement of radiation because some of the energy may come from the surroundings. Therefore the temperature of the crystal should be very low. Liquid nitrogen is usually used to cool down the semiconductor crystal (Eschenauer et al, 1994; Konya J, 2012). The most commonly used semiconductor detector and for the purposes of this study is the High Purity Germanium detector (HPGE), mainly for its high resolution. This is in spite of its very low efficiency of 36% relative to sodium iodide scintillation detector which is known for its high efficiency and poor resolution (Fayazi, 2005).

2.8 Gas ionisation detectors

Gas ionisation detectors consist of a gas-filled chamber with two electrodes; known as anode and cathode. The electrodes may be in the form of parallel plates (Parallel Plate Ionization Chambers: PPIC), or a cylinder arrangement with a coaxially located internal anode wire. An electric potential is applied between the electrodes to create an electric field between them. This generates a polarisation current in the chamber and also prevents the fill gas from becoming saturated. It only uses the discrete charges created by each interaction between the incident radiation and the gas, and does not involve the gas multiplication mechanisms used by other radiation instruments, such as the Geiger-Muller counter or the proportional counter (Wigner, 2004).

2.9 Naturally Occurring Radioactive Materials (NORMs)

There are radioactive elements that occur naturally on the earth's surface and are called the naturally occurring radioactive materials (NORMs). They are nuclides and elements that exist naturally at or near the earth's surface. NORMs are defined by the International Atomic Energy Agency (IAEA) as radioactive materials that contain no significant amounts of radionuclide other than naturally occurring radionuclides (IAEA, 2007). The three main categories of NORMs are cosmic rays, primordial radionuclides and the secondary radionuclides. This study focuses on the primordial NORMs. According to the oil and gas production (OGP) report, 2008, primordial radionuclides came from the thermonuclear reaction in the stars from the exploration of the supernova and the cloud when the sun and the solar system were created and became part of the earth's crust. The earth is naturally radioactive, and about 90% of that radiation comes from the NORMs (Hossain et al, 2010). These NORMs include Uranium-238 (^{238}U) and 235 (^{235}U), Thorium-232 (^{232}Th) and Potassium-40 (^{40}K). From these four natural radionuclides the commonest radionuclides that are available in considerably high concentration near the earth surface are ^{238}U, ^{232}Th and ^{40}K (Modisane, 2005). These NORMs decay to form other nuclides, which also decay to other nuclides forming a decay chain. Most naturally occurring radioactive materials and many fission products, undergo radioactive decay through a series of transformations. These series of decay will then leave long chain of radionuclides which also decay until the stable radionuclide. The series of nuclides from the parent to the stable radionuclide is called a decay chain (John et al, 1996). A stable nuclide is a nuclide that does not undergo radioactivity (Konya and Nagy, 2012).

The decay of NORMs has been grouped into series' that include all the decay products in the decay process. There are four different decay series namely uranium series, actinium series, thorium series and potassium 40. Figure 2.6 shows an example of the thorium and the uranium series and their progenies. A full table of the decay series with the main gamma lines are shown in Annexure 1.

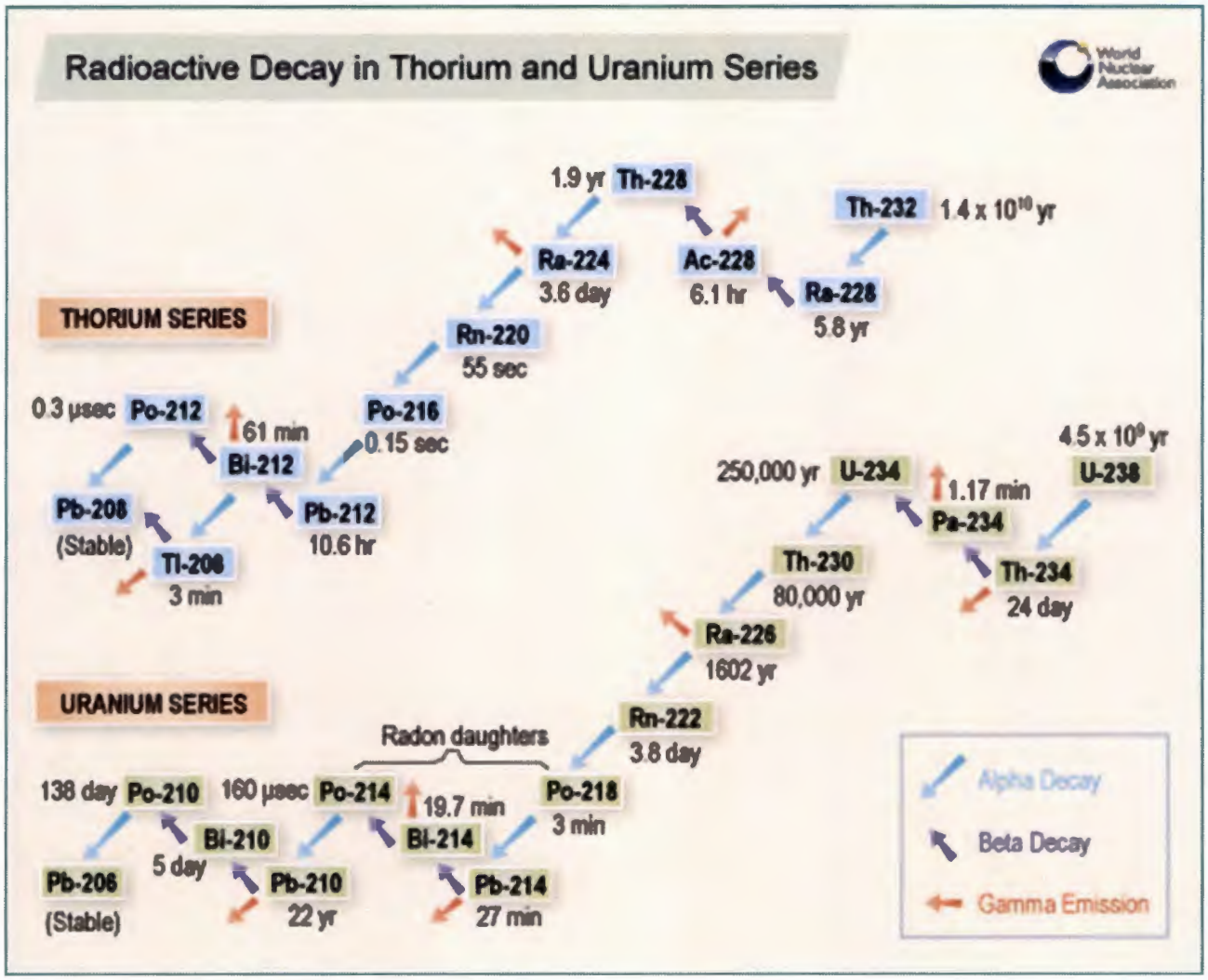

Figure 2.6: decay series for Thorium and Uranium

2.9.1 NORMs in mining

In general NORMS are available in very low concentrations in the soil surface (Modisane, 2005) and major concern comes when their concentrations are elevated since their effect on the environment depends their concentrations. Elevation of NORM concentrations can be done either by human practices like mining or by natural processes like earth quakes, landslides and sometimes even wind (Nour et al, 2005). Mining is one of the major causes of elevation of the NORM concentrations on the earth's surface. This is usually from the waste generated from the mining activities. This waste is usually deposited as mine tailing storage facilities (TSF). These mine tailings also known as mine dumps are the ones that have elevated NORM levels.

Many studies have been done on the measurement of naturally occurring radioactive elements in mining areas in the world. In Nigeria, in the Jos region, a mine tailing storage facility was analysed by Musicale, Anoka and Bologun. They concluded that the activities of Ra- 226 and Th-232 were much higher than the recommended average limit given by UNSCEAR, 2000 in the mining sites and even at 500 m away from the mining site (Musicale et al, 2011). The radioactive levels in the place were believed to have been elevated by the mining that had been done in the area for a very long time.

Another study was done in the Hirsa district of Haryana in India on the mine tailings of the different areas in the region. The results were analysed and the doses to the public were calculated. The results showed that the activity concentrations of the area were slightly higher than those that are given in the UNSCEAR, 2000, limits, even though the dose to the public was calculated and the hazard index showed no real need for the tailings to be rehabilitated (Kensal et al, 2012). Another study was done in Egypt in the Nile basin. Although here, it was not only mine tailings that were being investigated, they were reported to have slightly higher radiation than the world averages that are reported by the UNSCEAR, 2000 limits (Nour et al, 2005).

Studies in Poland which included almost all the mining areas in Poland were also done by Skubacz, and Melkino. They reported to have found levels of radiation higher than the world averages (Skubacz, and Melkinov, 2004). Zambian mines were also reported to have a high Uranium levels compared to world averages (Hayumbu et al, 2004).

A study by Frank Winde and Abraham de Villiers, in the Witwatersrand basin in 2002, showed that the gold mining area has a very high level of uranium pollution. They also concluded that the pollution was of an extra ordinary spatial dimension (Winde and De Villiers, 2002). This was also confirmed by Turton, in 2012, in an article entitled, "South Africa paying the price of gold", where he mentioned that the problem of radiation contamination from gold mining in South Africa especially the Witwatersrand basin is big and might stay for a long time (Humanitarian news, 2004)

There are many more other studies that have been done especially on the gold mining region in South Africa and most of them show that gold mining is associated with NORM pollution (Humanitarian News, 2004; Wendel, 1998). There are also environmental studies that have been done on the soil and the water sources from Princess Mine Dump which show that heavy metals found there (Ngigi, 2009). These different studies therefore have motivated the need for a radionuclide survey of Princess Mine Dump to investigate the amount of radionuclides found in the dust particles in the nearby communities.

Although Princess Mine Dump is an old mine tailing for gold mines, literature doesn't show any radioactivity studies that were performed on this tailing. This therefore makes it prudent to investigate the radioactivity of the tailing, by identifying, the different radionuclides present and the potential hazard the dump poses to the public, especially the communities living next to it.

2.9.2 Tenorms

According Environmental Protection Agency, rocks and soil contain natural radioactivity, which also dissolves into ground water. The occurrence of these "naturally occurring radioactive materials" (NORM) differs throughout the world, and may be more or less likely given the types of rocks and minerals in a particular area. NORM contributes a part of the natural 'background' exposure from radiation (EPA 2013).

When resources are extracted from the earth, the natural radioactive material comes with those resources. In processing the desired resource, the radioactive material is removed and becomes a waste (EPA 2013). The radioactive wastes from extraction and processing are called "Technologically Enhanced Naturally Occurring Radioactive Material" (TENORM) because human activity has concentrated the radioactivity or increased the likelihood of exposure by making the radioactive material more accessible to human contact (EPA 2013).

The most common naturally radioactive elements are uranium, thorium, and radium. Common sources of TENORM waste are mining and mineral processing, oil and gas production, and drinking water and wastewater treatment (EPA 2015).

2.10 Princess Mine Dump

Princess Mine Dump is located in Roodepoort, in the Gauteng region of South Africa. This region is well known for gold mining, and has been associated with elevated uranium concentration levels, due to mining activities (NNR report, 2008). It is located next to a human settlement, called Davidsonville. The image in figure 2.7 shows the south side of the dump.

Figure 2.7: A side view of Princess Mine Dump (Ngigi, 2009)

High winds which blow in the region, especially before the onset of spring rains, result in wind-blown tailings dust being generated from the dump to the nearby communities of Victory Park and Davidsonville (Ngigi, 2009). An article that was published by Zelda Venter for IOL-new online states that the mine dump was created by a number of companies that no longer exist, it forms an L shape and Victory park was developed inside the shape in the early 90s (Venter, 2006). Figure 2.8 shows

Princes mine dump (cream white in colour), with Victory park and Davidsonville near the dump. This area is in the Witwatersrand basin, and as the previous studies of this area have shown, it has a very high level of radioactivity. It is a course for concern when a mine dump has been left un-rehabilitated.

Figure 2.8: An aerial view of Princess Mine Dump and its surrounding areas

2.11 Radiation equilibrium

Figure 2.6 shows decay series' of uranium and thorium and the parent decays into daughters which end with a stable nuclide. When these decay series' take place in a closed system therefore, an equilibrium condition is reached with time. The decay rates are given by equation (11) below

$$\frac{dN}{dt} = \lambda_1 N_1 = \lambda_2 N_2 = \lambda_3 N_3 \ldots \quad (11)$$

and from equation two, λ is a function of the half-life. The longer half-life determines when equilibrium will be reached. Radiation equilibrium is very essential in gamma spectroscopy (discussed in detail in section 2.5); it can be used to calculate activities of nuclides that cannot be measured using the detectors. There are two types of equilibrium which are transient and secular equilibrium.

2.11.1 Secular equilibrium

Secular equilibrium is a steady state condition whereby the parent nuclide and its daughter have equal activities (Davies, 2010). If the parent has a very long half-life compared to its daughters in a decay chain, the activities of the natural radio isotopes can be measured and the concentration of the parent can be calculated from that of its daughters. For secular equilibrium to be assumed the ratio of $\lambda_{parent}/\lambda_{daughter}$ should be less or equal to 10^{-4}. This means that $\lambda_{parent} << \lambda_{daughter}$, therefore, to calculate the concentration of the parent the relation in equation 12 is used.

$$N_p\lambda_p = N_d\lambda_d, \qquad (12)$$

Where; N_p and λ_p are the number of atoms in a given sample and the decay constant of the parent, respectively, while N_d and λ_d are the number of atoms in the same sample and the decay constant of the daughter, respectively (Davies, 2010). Figure 2.1 shows graphs that indicate secular equilibrium. These graphs show the activity of the daughter nuclide and parent nuclide with time. As can be seen the activities after a certain long time (t) they then become equal. Secular equilibrium is concept very important in NORM calculations for extrapolating for parent activity from daughter activity or vice versa (Cheng et al, 2000).

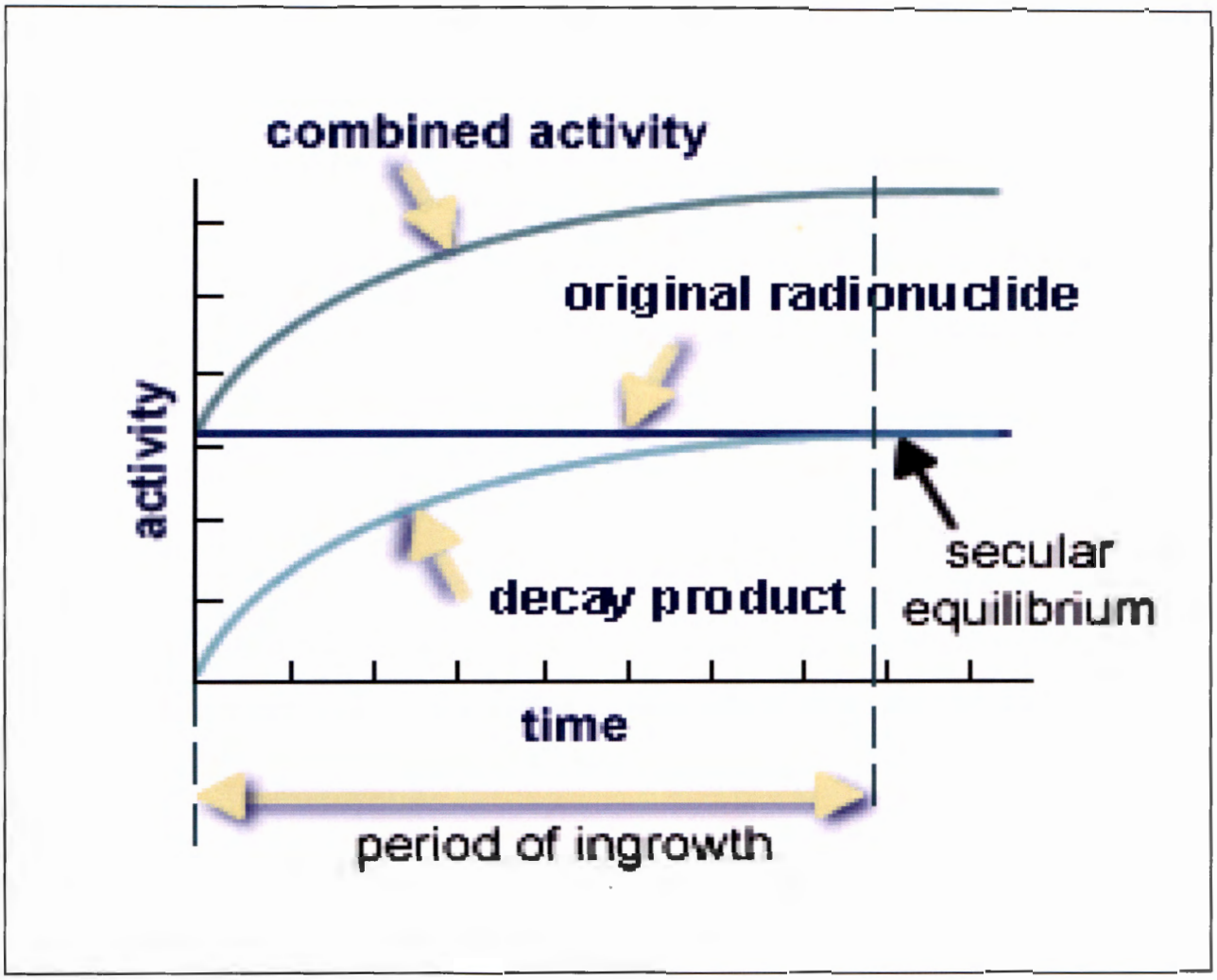

Figure 2.9: secular equilibrium (http://www.epa.gov)

2.11.2 Transient equilibrium

In transient equilibrium, a steady state condition between the parent and the daughter and parent nuclide exists like in secular equilibrium but the parent and daughter nuclides do not have the same activities but rather they decay at the rate of the half-life of the parent nuclide (L`Annunziata, 2003). With the condition $\lambda_{parent} << \lambda_{daughter}$, an added condition lies in the fact that the ratio $\lambda_{parent} / \lambda_{daughter}$ should fall with the limit $1 \geq \lambda_{parent} / \lambda_{daughter} \geq 10^{-4}$. Figure 2.10 is a graph showing transient equilibrium.

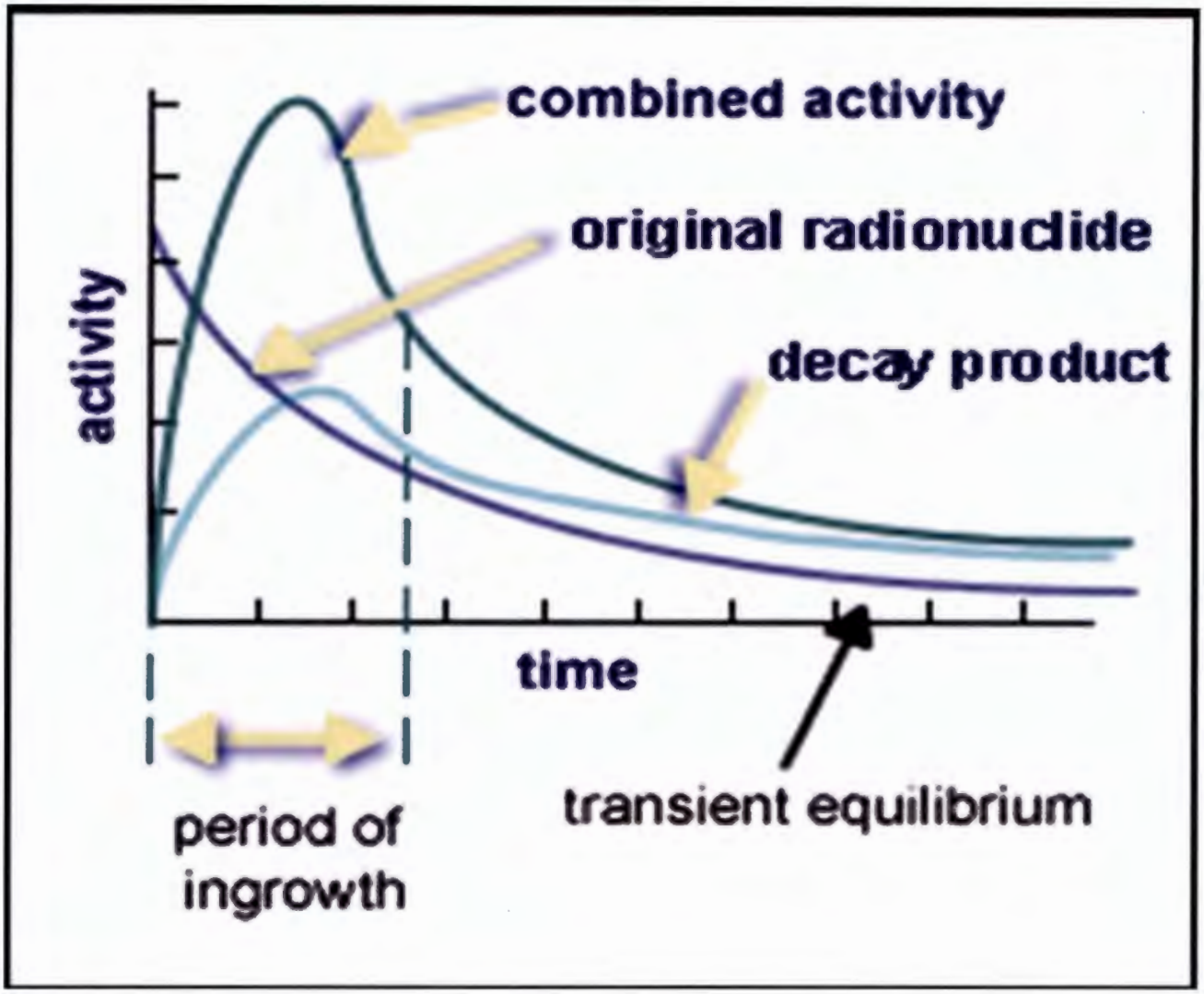

Figure 2.10: Transient equilibrium (http://www.epa.gov)

2.12 Mobility of NORMs in sediments

For solid sources like the ores of uranium and thorium, the mobility of the sediments depends of the solubility and dissolution or leaching (Battachryya, 1998). Concentration variations are induced by local differences in sediment properties leading to interactions such as adsorption to clay or by physical selection processes like settling of contamination at the inner bed due to velocity differences (Van der Graaf et al, 2007). In such a case a radionuclide will be assumed to disperse and is similarly affected by transport and interaction processes. A prerequisite for the dispersed present radionuclide is that the compound should be mobile and the mobility of the compounds in freshwater sediments is restricted by their adsorption to the sediments.

For uranium; it occurs as the aqueous uranyl (IV) ion (UO_2^{2+}) under standard enviro-toxic conditions. This ion is very mobile and through its mobility, it can be distributed over large areas. The adsorption of uranium is low at low pH values and increases with pH reaching a plateau between pH 5 and 8. It then decreases as the pH goes higher again (Van der Graaf et al, 2007).

For thorium; it exist as a Th (IV), and its mobility is limited by the formation of its insoluble hydroxide $Th(OH)_4$ (Xan der Graaf et al, 2007). Thorium has a strong affinity towards suspended particles. This makes it a more stagnant nuclide because even when it becomes mobile it gets reabsorbed.

Most radionuclide ions bind to solid surfaces by a number of processes often classified under a very broad term called sorption. The behaviour and ultimate radiological impacts of radionuclides in solids are controlled by their chemical form and speciation, which in turn affects their mobility, residence time within the soil rooting time and uptake by biota. Partitioning of radionuclides between water and suspended matter is described in terms of the distribution coefficients (K_d) expressed as concentration ratio between the particulate phase and the dissolved phase under equilibrium conditions (Ciffroy et al, 2009). K_d values are usually used in the simulation of the transport of pollutants in rivers (Monte et al, 2010).

Radionuclide sorption on solid phase is quantified using the distribution coefficient (K_d). This is also used for assessing the overall mobility and likely time of stay of the radionuclides in solids (IAEA, 2007). The distribution coefficient is based on the hypothesis of a reversible and rapid equilibrium between the dissolved (C_w) and the adsorbed phases of the radionuclide as shown in equation 13:

$$K_d = \frac{C_s \ \textit{activity concentration in solid phase}}{C_w \ \textit{activity concentration in liquid phase}} \left(\frac{Bqkg^{-1}}{Bq\,L^{-1}}\right) \qquad (13)$$

Partition coefficients describe the distribution of contaminants between water and sediments and they indicate their relative mobility (Fuhrman et al, 1997). They are mainly used in the modelling of transport and distribution of radionuclides in environmental systems that contain fluids and particulates.

2.13 Biological effects of radiation

Radiation can be ionising and non-ionising. Non ionising radiation is normally of little concern since no studies so far have shown any significant effect unlike ionising radiation. When the human body is exposed to ionising radiation, either from external or internal sources, ionisation and excitation of atoms, molecules and even electrons can be produced. Consequently, the interaction of radiation with biological organisms can result in the damage and death of living cells and/or the mutation of genetic material. The variation of the biological effects of radiation depends on types of radiation, its energy which is transferred to the irradiated parts of tissues and organs during the exposure time. The quantification of the amount of ionisation which occurred and the energy absorbed by particular cells associated with biological effectiveness can be considered in terms of radiation dosimetry (Greening, 1985).

2.13.1 Radiation dosimetry

The roentgen

This is a legacy unit for the measurement of X-rays and gamma rays exposure of up to 3 MeV. It is defined as the amount of ionisation that X and γ - rays produce in air. This therefore means that 1 roentgen = 1esu of electrical charge produced in $1cm^3$ of air. The SI unit for the roentgen is the C/kg.

$$1R = 1\frac{esu}{cm^3}2.58 \times 10^{-4}\frac{C}{kg}, \qquad (14)$$

This unit is only an exposure unit and is limited only to energy photons like the X and γ - rays. Also it's only useful for a limited range of energies (Stabin, 2007).

Absorbed dose

Due to the limitation of the roentgen as a mere exposure unit, the absorbed dose is a much more relevant unit as it describes the biological effect of radiation. The absorbed dose is a measure of the energy deposited into the body. It is mathematically defined as 1 joule of energy deposited per 1kg of tissue. The unit of the absorbed dose is the Gray (Gy), this is equal to 1joule (J) of energy deposited per 1kg of irradiated target. Some text though use the radiation absorbed dose (rad) as a unit for absorbed dose. This unit is equal to 100 ergs of energy per gram. It follows therefore that:

Since$1J = 107\ ergs$,

$$1Gy = 1\frac{J}{kg} = \frac{10^7 erg}{10^3 g} = 10^4\frac{erg}{g} = 100rad$$

or $1rad = 0.01Gy$

The energy absorbed is not the only factor that is to be considered when dealing with the radiation dose. The type of radiation is also very important as different types of radiation have different effects on different tissue. Therefore relative biological effectiveness (RBE) of the radiation was introduced as a dimensionless quantity of the amount of absorbed dose relative to the amount of absorbed radiation. This hence caters for the biological response that is produced by the different types of radiation. These RBEs have been normalised, to minimise complications, to radiation weighting factors, and table 2.1 shows the different weighting factors as provided by the ICRP (ICRP 92, 2003).

Table 2.1: Radiation weighting factors for different radiation (Allen et al, 2012)

Type of radiation	Energy range	Weighting factor, w_R
Photon, electrons positrons and muons	All energies	1
neutrons	<10 keV	1
	> 10keV to 100 keV	10
	>100keV to 2 Mev	20
	>2 MeV to 20 MeV	10
	>20 MeV	5
Protons	<20Mev	5
Alpha particles, fission fragments, non-relativistic heavy nuclei		20

Equivalent and effective dose

As has been observed the absorbed dose (D) alone cannot describe the effect radiation on the target material. Therefore, for a more defining quantity, the equivalent dose (H_T) was introduced. This is defined as the amount of dose ($D_{T,R}$) absorbed over a tissue or organ (T) due to radiation (R). This quantity is given by equation (15)

$$H_T = \sum_R W_R D_{T,R}, \qquad (15)$$

The unit for expressing the equivalent dose is the Sievert (Sv). The Sv is used to express the equivalent dose while the absorbed dose is expressed in units of Gy. This therefore means that one Sv also is equal to one Joule per kilogram. An older unit for the equivalent dose is the rem which is 100 times smaller than the Sievert, ($1Sv = 100rem$). In addition to the sensitivity of the biological systems being sensitive to the type of radiation also the different organs react differently to radiation, i.e. the same type of radiation can produce different effects on different organs. This then called for other relative response quantities for the tissue, which takes to account for the different reactions for different organs to radiation. Also developed, is simple tissue weighting factors for the different organs or tissues as can be shown in the table 2.2.

Table 2.2: Tissue weighting factors (Allen et al, 2012)

Tissue or organ	Tissue weighting factors (w_T)
Gonads	0.20
Colon	0.12
Lung	0.12
Red bone marrow	0.12
Stomach	0.12
Bladder	0.05
Breast	0.05
Oesophagus	0.05
Liver	0.05
Thyroid	0.05
Skin	0.01
Bone surfaces	0.01
Remainder	0.05

Also derived from the different tissue weigting factors, is a different quantity called the effective dose (E) (allen et al, 2012). The effective dose takes into account the tissue weighting factors and is given in equations 16 and 17

$$E = \sum_T W_T H_T, \quad (16)$$

Or

$$E = \sum_T W_T \sum_R W_R D_{T,R}, \quad (12)$$

2.13.2 Risk assessment

The radioactive hazard or risk that can be posed by NORMs in an area, can be determined by calculating the radium equivalent, using equation 18 and the absorbed dose rate at 1m above the ground level using equation 19 (Kansal et al, 2010). The radiation equivalent is calculated from the activity concentrations of ^{226}Ra, ^{232}Th and ^{40}K. The mathematical definition of the radium equivalent comes from the

assumption that 370 Bq/kg ^{226}Ra, 259 Bq/kg ^{232}Th or 4810 Bq/kg ^{40}K produce the same gamma dose rate (Ahmed and Arabi, 2005).

$$Ra_{eq} = C_{Ra} + 1.43C_{Th} + 0.077C_K , \quad (18)$$

Where; Ra_{eq} - is radium equivalent activity

C_{Ra} - is specific activity of ^{226}Ra

C_{Th} - is specific activity of ^{232}Th

C_k - is specific activity of ^{40}K

The absorbed dose rate at 1m above the ground can be calculated using the NORMs activity concentrations also shown in equation (19).

$$D(nGyh^{-1}) = 0.0417C_K + 0.46C_{Ra} + 0.604C_{Th} , \quad (19)$$

Equation 14 only caters for the external dose calculations (i.e. the calculation of dose from external exposure). Equation (20) therefore is for the calculation from the internal dose. These two parameters combined, will give the annual effective dose equivalent given by equation (21).

$$Yearly\ Dose = Yearly\ Consumption \times Specific\ Activity \times Dose\ Conversion\ Factor, \quad (20)$$

Sv / a] [Kg / a] Bq / kg] [Sv / Bq]

$$AEDE(Sv) = \text{ADRA}\left(\frac{nGy}{h}\right) \times \text{DCF}\left(\frac{Sv}{Gy}\right) \times \text{OF} \times \text{T(h)} , \quad (21)$$

Where AEDE – is the annual effective dose equivalent

ADRA – is the absorbed dose rate in air

DCF – is the dose conversion factor

OF – is the outdoor occupancy factor

T – is the time (Karahan and Bayulken, 2000).

The two equations i.e. equation 22 and 23 show the AEDE for outdoor and indoor, and the difference is the occupancy factor. The occupancy factor is the fraction of time spent by the single person who is in a certain place the longest (shielding design, 1999). This means that the indoor occupancy factor for this study in not relevant as this study is about a mine dump and it can never be indoors. Only the outdoor occupancy factor can be used.

$$Indoor\ (nSv) = Absorbed\ Dose(nG/y) \times 8760(h) \times 0.8 \times 0.7(Sv/Gy), \quad (22)$$

$$Outdoor\ (nSv) = Absorbed\ Dose(nG/y) \times 8760(h)\, x\, 0.8 \times 0.7(Sv/Gy), \quad (23)$$

Another parameter that is normally used to calculate the risk that is posed to the environment is the hazard index (H_{ex}) which can be calculated using equation 24.

$$H_{ex} = \frac{C_{Ra}}{370} + \frac{C_{Th}}{259} + \frac{C_K}{4810}, \quad (24)$$

The hazard index determines the habitability of an area radiologically. The limit that is given by the USCEAR, 2000 is unity. This means that if the hazard index of a particular area exceeds unity then that area is not good habitation.

2.14 Inductively Coupled Plasma Mass Spectroscopy (ICP-MS)

ICP-MS stands for the inductively coupled plasma- mass spectrometry. This is an elemental analysis system, which is both qualitative and quantitative. The system involves two known techniques, merged to improve accuracy. These are the inductively coupled plasma system (ICP) and the mass spectrometer (MS), as can be shown in Figure 2.11. The ICP system is just for the atomisation of the sample in question. It uses a nebulizer, which will turn the liquid sample into a spray and the presence of argon which is rotated at very high frequency to form a plasma, which when it comes into contact with the sample it atomises the sample. The mass spectrometry (MS) system is attached at the end of the ICP, and is mainly for the separation of the different ions. The MS system has a magnetic field and an electric field attached perpendicular to each other and these bend the path of the atoms as they enter the system. The radius or the arch is dependent on the mass of the atoms. The atoms are separated, as they move to the detector, and then the computer software using the calibration standards can analyse the different atoms in the sample (Gross, 1999).

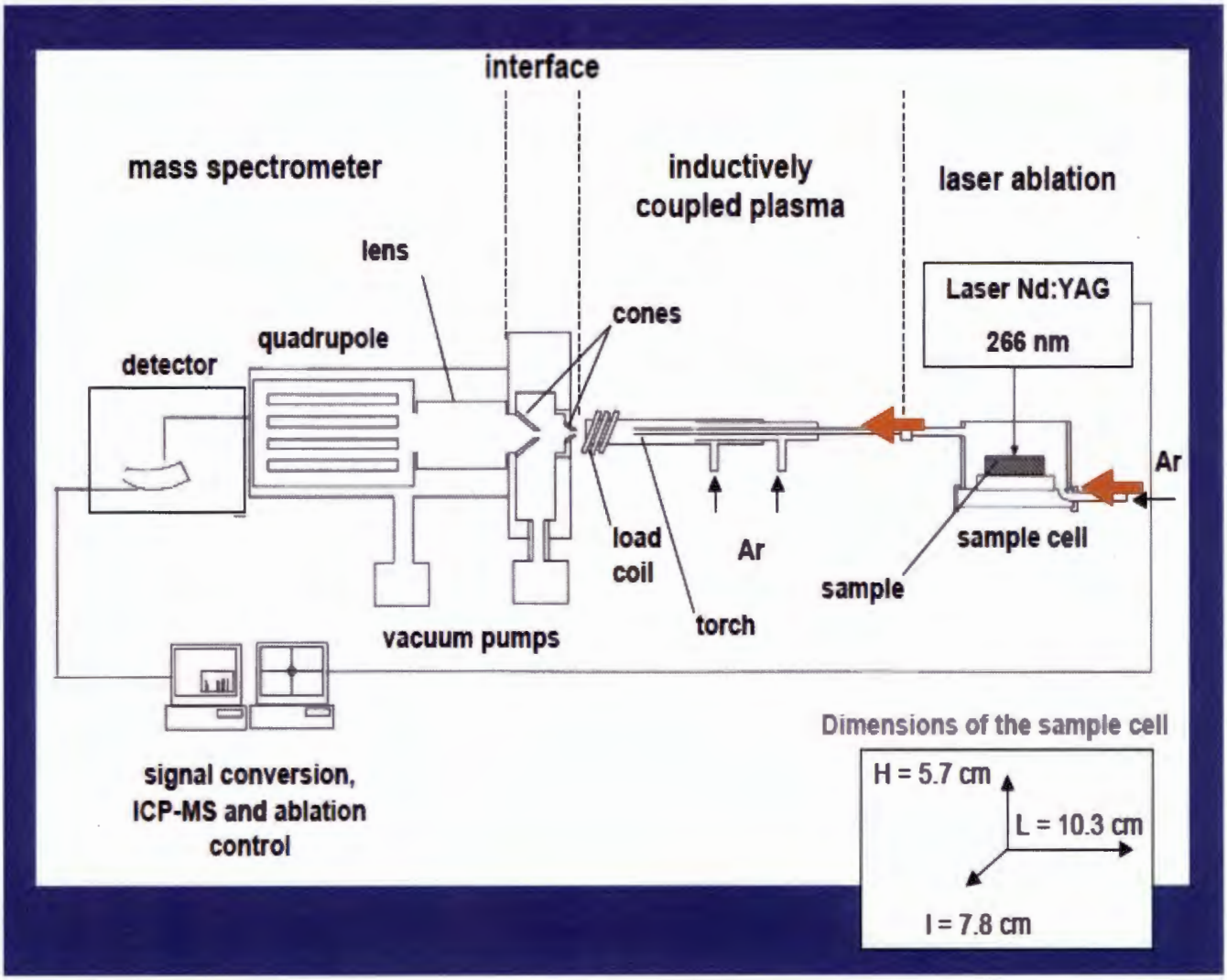

Figure 2.11: A schematic set-up for ICP-MS

CHAPTER 3: METHODOLOGY

3.1 Introduction

The study area is situated at the upper Klip River catchment area, at Longitude 27 55 00 E and Latitude 26 09 30 S. It is located at the Roodepoort West area and about 10 kilometres southeast of Krugersdorp. According to Venter, 2006, Princess Mine Dump was created by a number of mining companies that no longer exist. It forms an L shape and Victory park was developed inside the shape in the early 90s (Venter, 2006). Figure 2.8 shows Princes Gold mine dump (cream white in colour), with Victory park and Davidsonville near the dump. The project focused on identifying radionuclides in the mine dump, measuring their activity concentrations, measures the amount transmitted to dust particles around the area and calculates the approximate potential radiological hazard that the mine tailing dust poses to the public especially the neighbouring communities.

3.2 Sample collection

The points were selected in such a way that the sample points were approximately 10 metres apart from each other. The sampling points were marked using letters A to Z, as shown in figure 3.1. At each point two samples were taken; one at 10 cm below surface and the second at one metre below the surface. Princess Mine Dump was mapped in such a way that selected points were representative of the entire volume. For ease of identification the sampling points were marked with a GPS and labelled A to Z as shown in Figure 3.1.

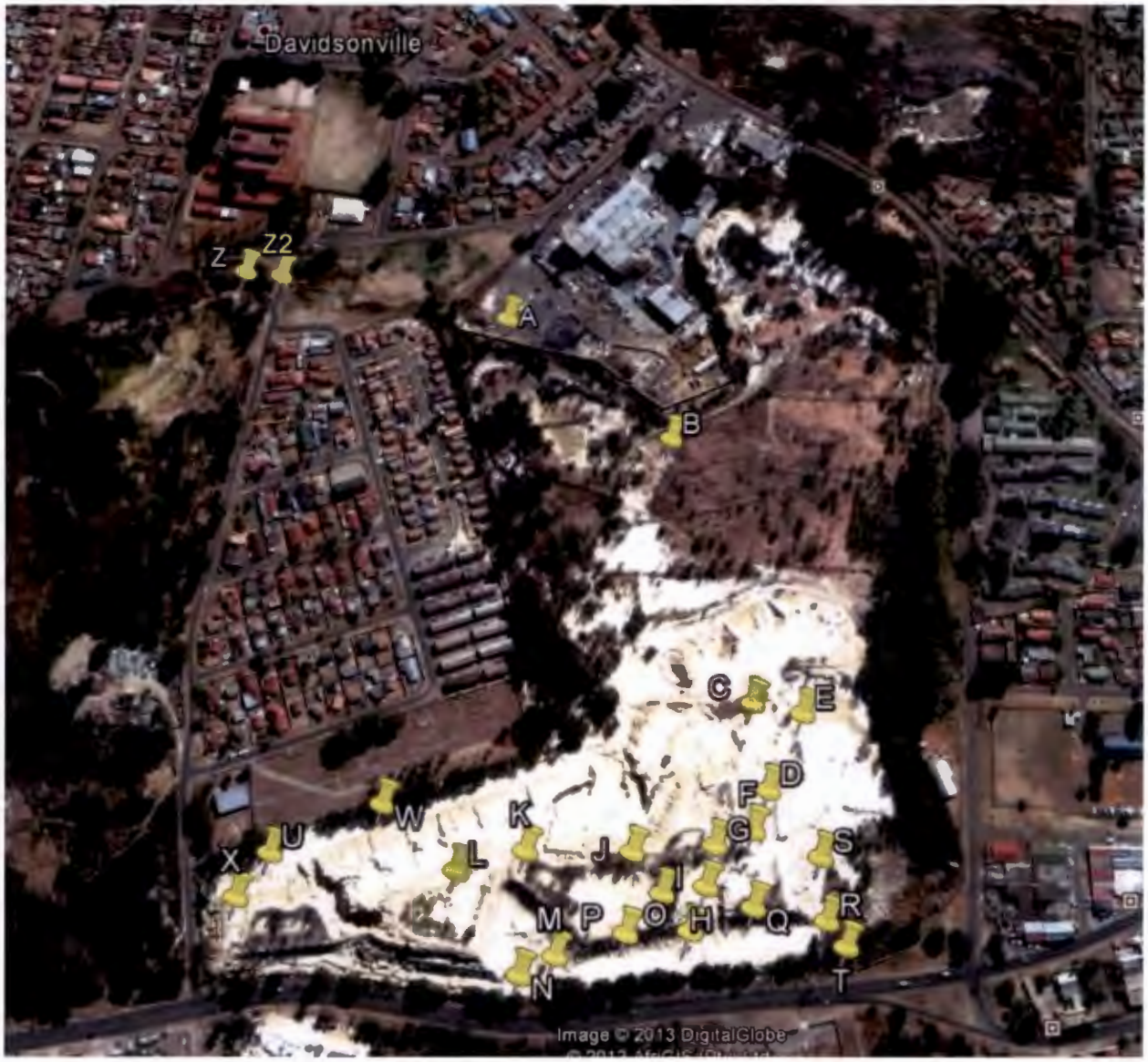

Figure 3.1: An Aerial view of Princess Mine Dump showing also the different sampling points (shown in yellow)

The samples were dug or extracted using a manual auger with 10 cm diameter, as shown in figure 3.2. The volume of each sample collected was more than 1000 cm^3, enough sample to fill the marinelli beaker. The samples collected from the top and bottom soils were given the second names one and two, respectively. For an example names A1 and A2 referred to samples at the top and bottom of GPS point A, respectively. All points were named in the same pattern.. Samples were collected into heavy duty plastic bags, tied using cable tires to avoid cross contamination and marked for identification before shipment to the laboratory for analysis.

Figure 3.2: A manual auger for extraction of soil samples (AMS samplers)

3.3 Sample Preparation

At the laboratory, CARST, the samples were prepared in line with the analytical equipment to be used. The samples were air dried, organic materials, rocks removed and carefully separated with a sieve to ensure uniformity in the sample before transfer into the marinelli beakers. The geometry of each marinelli beaker was 88 mm inner diameter and 130 mm outer diameter. These dimensions made the beaker fit when covering the detector and also fit in the lead shield, as all the measurements were to be done in a lead shield. After the samples were transferred into the marinelli beakers, they were closed, sealed using masking tape, for 24 days to allow

soil samples to attain secular equilibrium between radium-226 (^{226}Ra) and its progenies.

3.4 Calibration of the instrument

Instruments are calibrated regularly in order to achieve good results. In general to calibrate is to determine or rectify the graduations of any instrument giving quantitative results. Calibration of instruments differs with each instrument and is dependent on the principle of operation of each instrument (Harald, 1992). In gamma spectroscopy there are two types of calibrations that need to be performed which are the energy and efficiency calibrations and as discussed earlier.

3.4.1 Energy calibration for gamma spectroscopy

Energy calibration of the instrument was done using a ^{133}Ba and ^{152}Eu mixed source. The mixed source was prepared in the laboratory using a ^{133}Ba and ^{152}Eu powdered standard that had been prepared at NECSA. The powdered standard of ^{133}Ba and ^{152}Eu source with activities, 5.97 kBq and 13.06 kBq respectively was mixed with sample soil from Princess Mine Dump. This was done to make sure that the absorbing matrix was almost similar to soil samples that were being analysed. The source was run for three hours in the germanium detector. Three trials were done and three gamma energy lines were chosen with their channels numbers noted. These gamma lines were chosen such that they covered the whole spectrum. The standard library was used to match the channel and corresponding energy according to the calibration source. Figure 3.3 shows the energy calibration curve the calibration equation and the correlation coefficient (R^2).

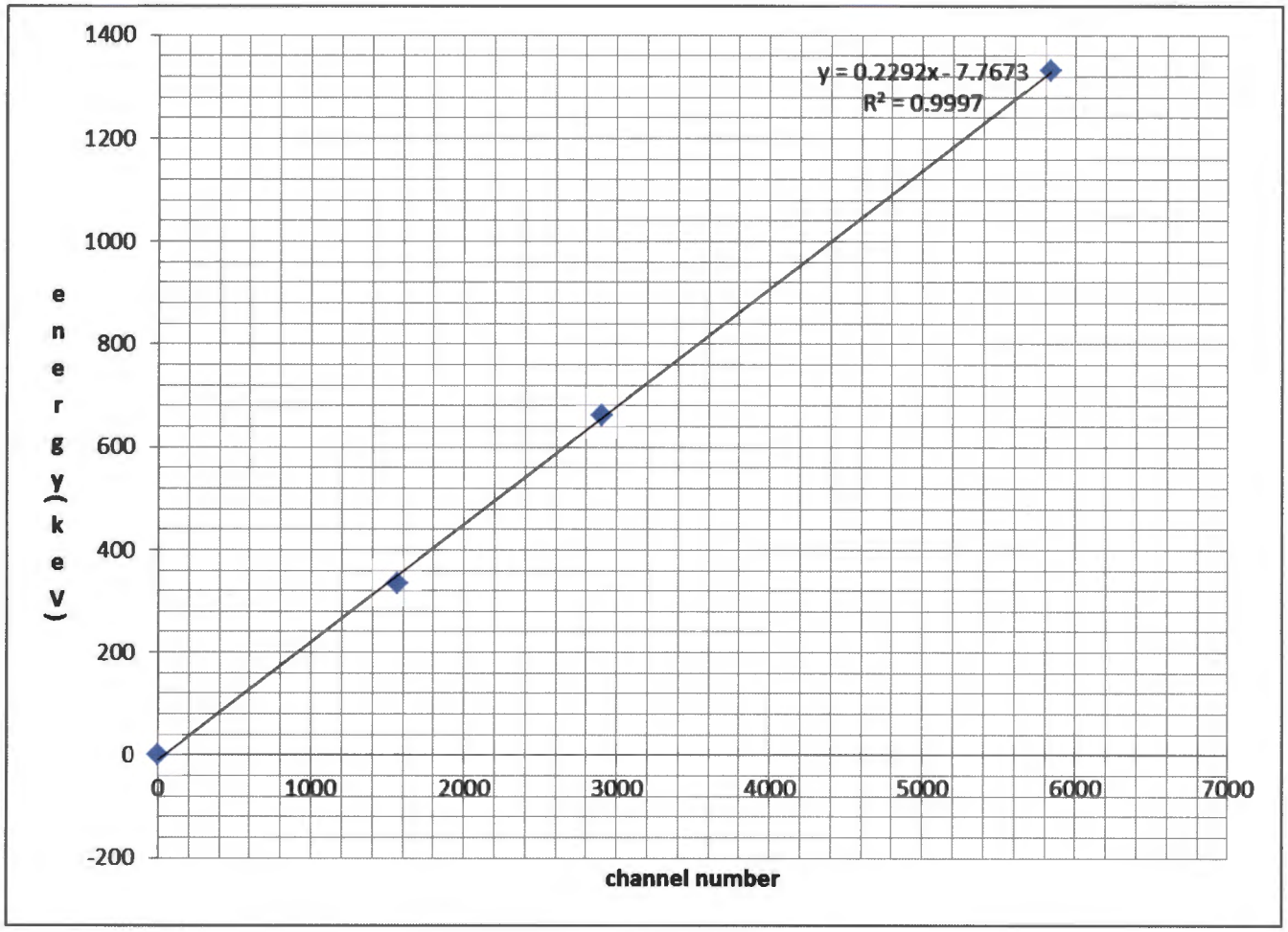

Figure 3.3: The energy calibration curve

3.4.2 Efficiency calibration for gamma spectroscopy

The principle of gamma spectroscopy is based on the measurement of an output pulse for each radiation that interacts with the active volume (which can be any active centre in the different types of radiation mention in section 2.5 that can be the gas ionisation centre, the scintillator or the semiconductor depending on the type of detector that is being used) of the detector. Gamma rays can travel longer distance even in the active centres before they interact with the active volume; therefore the efficiency of detection is not 100% (Daraban, 2012). The efficiency equation is shown below

$$\varepsilon = \frac{N_r}{N_\lambda} \qquad (25)$$

Where ε - is the efficiency of the peak

N_r - is the net count rate reported by the detector

N_λ - is the gamma emission rate

The efficiency calibration therefore corrects the full energy peaks for the undetected gamma interactions. In this study the ^{133}Ba and ^{152}Eu was again used for the efficiency calibration. After the acquisition or the running of the source with the gamma spectrometer, the following lines were considered for the two radionuclides:

For ^{152}Eu – 40.11 keV, 45.37 keV, 121.77 keV, 367.79 keV, 1085.88 keV and 1408 keV
For ^{133}Ba – 53.14 keV, 80.98 keV and 160.6 keV

These energies cover almost the entire spectrum which is good for the authenticity of the calibration process (Osvath, 2008). The ratios of the measured energy to the true energy value for each of the gamma lines was calculated and plotted against the energy. Then a regression using excel was performed measure or calculate the efficiency of the detector and the results plotted in the graph in figure 3.4.

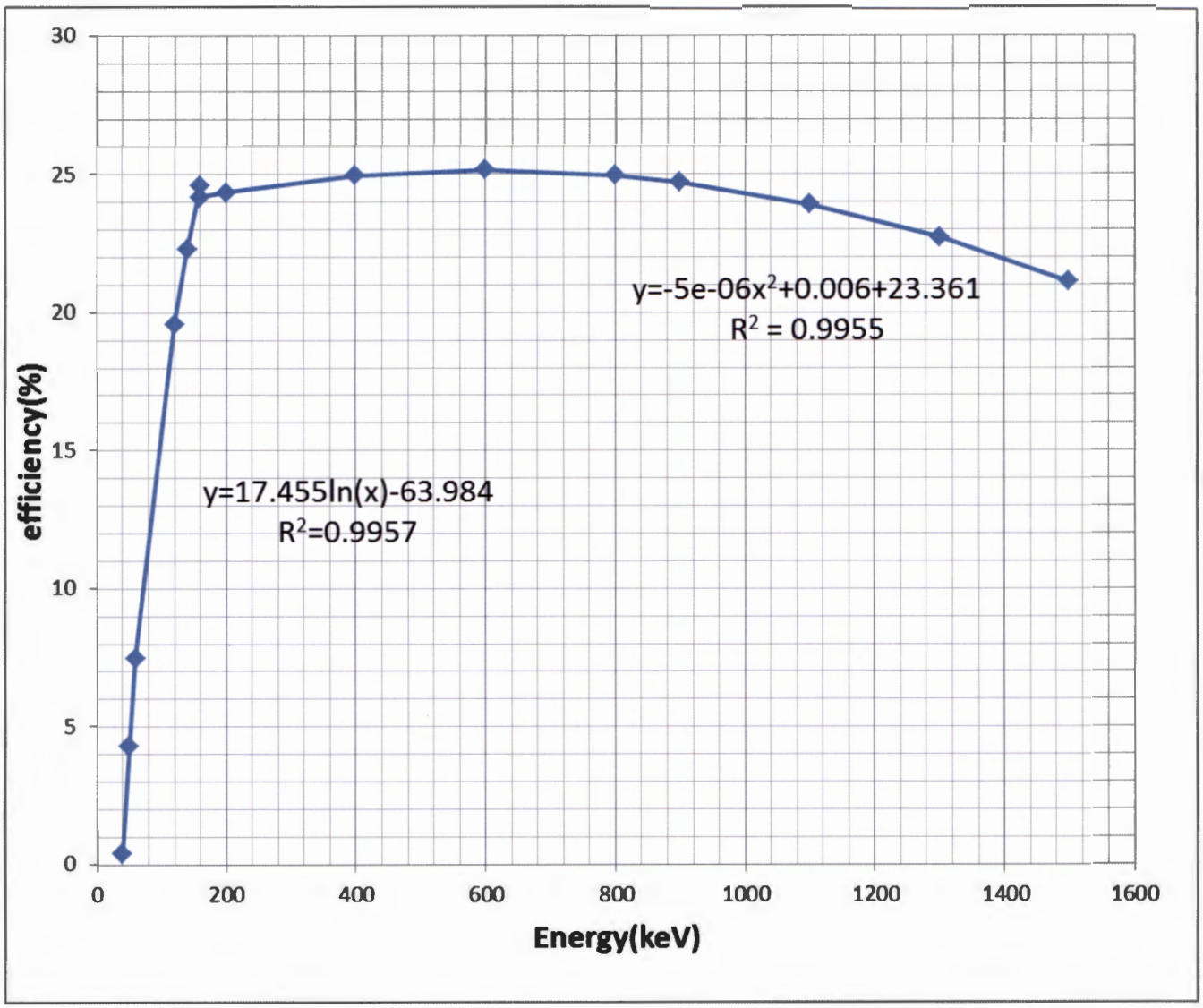

Figure 3.4: Efficiency calibration of the high purity germanium detector GCD-35 190

3.4.3 Calibration of the ICP-MS

For the calibration of the ICP-Ms, standard solutions were used which contained elements were a representative of almost the whole range of the Periodic Table of elements. Calibration of the instrument is done every time the machine is started. ICP-MS does the calibration by running the standard a number of times until it gives the correct value as given in the certificate. The instrument is provided with the correct value of the concentration of the standard prior to running. When the measurement gives the correct value then the instrument gives the green light to start the running of the samples.

3.5 Data Acquisition

The data was acquired using high resolution based HPGe GCD-35 190 detector. The resolution of the detector is 120 keV at 1332 keV for ^{60}Co with efficiency of 36% compared to the sodium iodide detector. The detector was cooled with liquid nitrogen to keep the germanium crystal at the required low temperatures. The detector was placed in a lead shield (as shown in figure 2.5) to eliminate background (Varshini et al, 2008). A background spectrum was acquired first for 24 hours and the spectrum was saved as a blank. The blank was an empty marinelli beaker sealed with masking tape to make sure the conditions are the same as the samples. After running the blank/background spectrum the samples were placed on top of the detector and the data was collected for 24 hours in each sample. The data acquisition was carried out inside a lead shield to eliminate as much background as possible (Verplancke , 1992). A multichannel analyser that is operated with *win spec* software was used for the data collection. Win spec software is gamma spectroscopy data acquisition software. After the data acquisition was done each sample spectrum was saved in a file in readiness for analysis.

The next step was the analysis of the data which included the identification of the peaks and calculation of activities using the IDENTIFY software. Identify software is a software that is used in gamma spectroscopy to analyse activities and identify gamma lines using different libraries. The software subtracts the background and then each and every peak can be analysed. The analysis gives the results for the peak, which are energy, and also calculates the activity of the peaks.

CHAPTER 4: RESULTS AND DISCUSSION

4.1 Introduction

In this chapter the results and the data collected will be presented. The data analysis and the corrections of the data performed will be discussed. The analysis and the calculations for risk assessment will also be presented.

4.2 Results

Figure 4.1 shows a typical gamma spectrum for the soil samples from Princess Mine Dump displayed using IDENTIFY software. These were collected using the portable GCD-35 190 high purity germanium detector. The spectra for all the samples from princess dump and the background follow a similar pattern.

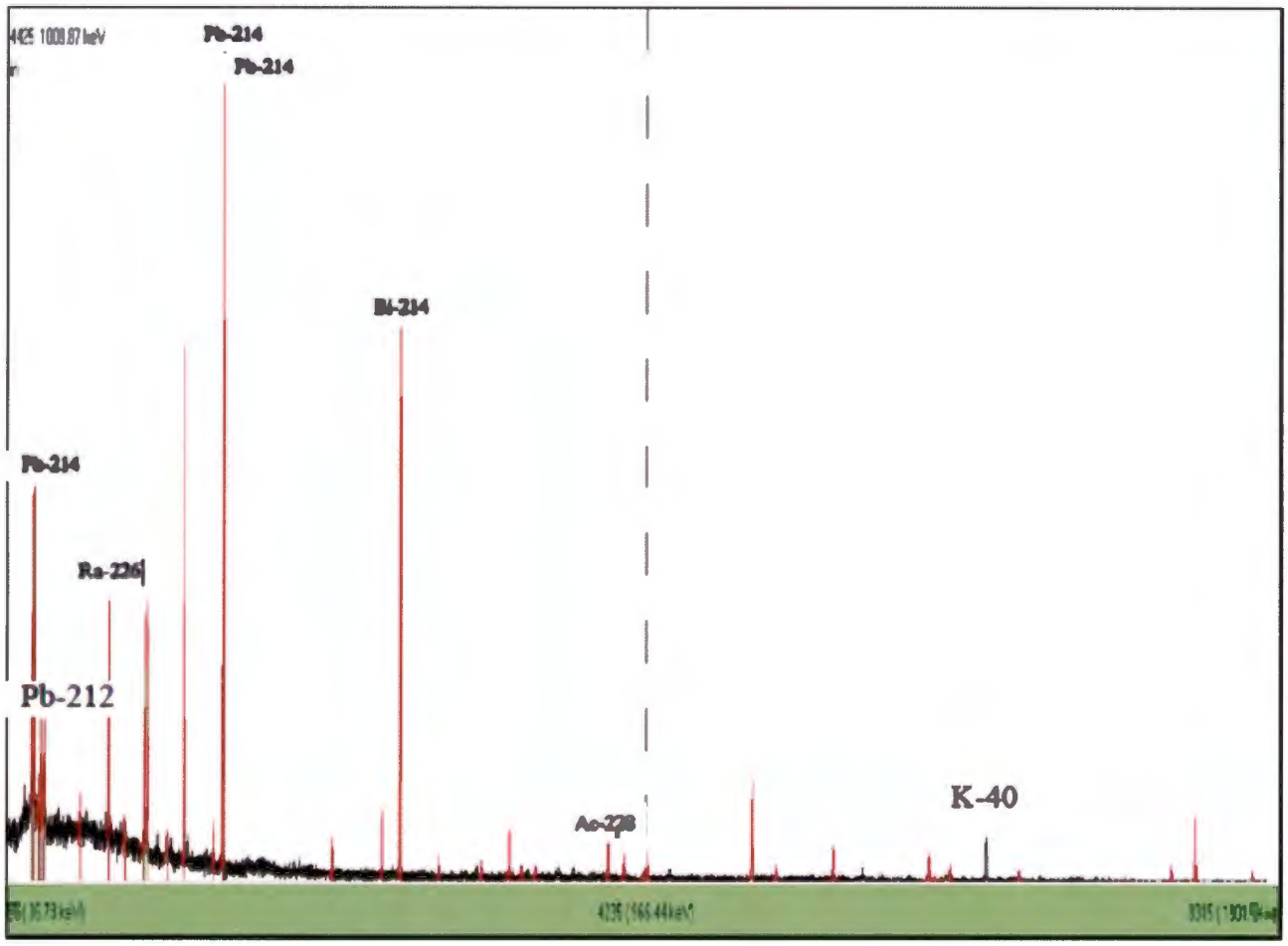

Figure 4.1: A typical gamma spectrum for a soil sample taken from Princess Mine Dump

4.2.1 Determination of radioactivity

The 42 soil samples were collected from Princess mine dump. The samples were sealed for 24 days to ensure that parent nuclides are in secular equilibrium with daughter nuclides. The sample holders were placed on top of the detector inside the lead shield. To minimise the statistical errors, data for each sample were collected for 24hours. The readings were also taken with an empty container on top of the detector to estimate the background radiation from the surrounding in the laboratory. The spectra were collected using win spec software and the analysis was performed using IDENTIFY software. Before the analysis was performed, each spectrum was corrected for the background. The activity of the parent nuclide was calculated by measuring the activity of the daughter nuclide. Figure 4.1 presents the typical spectrum of one the samples from Princess mine dump. The lower energies the spectrum is dominated by the ^{214}Pb peaks while the higher energies are dominated by the ^{214}Bi.

The 46.5 keV and 1460 keV for ^{214}Pb and ^{40}K gamma lines were analysed because they are very prominent in the spectrum. The 92.4 keV line for ^{234}Th was used to calculate the activity of ^{238}U, the 911 keV line for ^{228}Ac was used to calculate the activity of ^{228}Ra, the 351 keV was used to calculate the activity of ^{226}Ra and the 238 keV for ^{212}Pb which was used to calculate the activity of ^{228}Th by assuming that daugther nuclides are in secular equilibrium with parent nuclides. The average activities of each peak from the software were divided by the mass of each sample to obtain the activity concentrations for each radionuclide in each sample.

In Table 4.1 and 4.2 the activity concentrations for the soil samples taken at 15cm from ground level and the samples taken from 100cm deep are presented, respectively. The activity concentrations ranged from 108 ± 20 to 1300 ± 115 Bq/kg, 58.6 ± 15 to 271 ± 16 Bq/kg, 12.6 ± 0.5 to 50.2 ± 11 Bq/kg, 36.2 ± 3.0 to 485 ± 36 Bq/kg and 31.3 ± 4.7 to 148 ± 23 Bq/kg for ^{210}Pb, ^{238}U, ^{228}Th, ^{226}Ra and ^{40}K, respectively for the topsoil. The activity concentrations for the bottom soil (100cm below surface), ranged from 262 ± 8.3 Bq/kg to 1550 ± 195 Bq/kg, 49.8 ± 1.0 to 399 ± 9.5 Bq/kg, 11.0 ± 0.2 to 44.6 ± 0.8 Bq/kg, 112 ± 13 to 532 ± 57 Bq/kg and 31.3 ± 6.7 to 167 ± 44 for ^{238}U, ^{228}Th, ^{226}Ra and ^{40}K, respectively.

Table 4.1: Activity Concentration for the NORMs and their progenies Bq/kg for the soil samples taken at 15cm below ground level.

	^{210}Pb	^{238}U	^{228}Th	^{226}Ra	^{228}Ra	^{40}K
B1	1.08E+02	1.14E+01	2.01E+01	3.62E+01	1.72E+01	9.72E+01
C1	6.02E+02	1.15E+01	2.10E+01	1.38E+02	1.49E+01	9.07E+01
D1	5.00E+02	1.11E+01	1.90E+01	1.55E+02	1.54E+01	4.29E+01
E1	4.51E+02	1.36E+01	1.99E+01	1.37E+02	1.53E+01	1.39E+02
F1	4.78E+02	1.51E+01	2.33E+01	2.27E+02	2.03E+01	9.75E+01
G1	3.04E+02	9.20E+00	1.65E+01	1.43E+02	1.58E+01	9.12E+01
H1	8.34E+02	1.49E+01	2.12E+01	1.93E+02	1.67E+01	1.08E+02
I1	7.68E+02	1.84E+01	2.88E+01	1.92E+02	2.41E+01	1.40E+02
J1	1.11E+02	5.86E+00	1.26E+01	5.34E+01	1.04E+01	4.07E+01
K1	1.89E+02	1.14E+01	2.43E+01	1.68E+02	2.07E+01	7.18E+01
L1	4.36E+02	9.57E+00	2.20E+01	1.25E+02	1.82E+01	9.27E+01
M1	4.26E+02	9.72E+00	1.64E+01	9.95E+01	1.30E+01	4.94E+01
N1	1.30E+03	2.71E+01	3.97E+01	4.85E+02	2.20E+01	1.30E+02
O1	4.39E+02	6.74E+00	1.76E+01	1.75E+02	1.35E+01	6.74E+01
P1	7.42E+02	1.32E+01	1.65E+01	1.65E+02	1.49E+01	6.10E+01
Q1	4.83E+02	1.40E+01	2.22E+01	1.84E+02	1.77E+01	8.59E+01
R 1	3.89E+02	6.89E+00	1.87E+01	1.63E+02	1.72E+01	9.34E+01
S1	4.18E+02	1.08E+01	2.26E+01	1.35E+02	1.92E+01	1.48E+02
U1	7.91E+02	2.09E+01	3.79E+01	3.68E+02	2.38E+01	1.22E+02
W1	1.26E+03	9.60E+01	5.02E+01	4.13E+02	3.62E+01	9.57E+01
X1	2.99E+02	8.42E+00	1.39E+01	1.56E+02	1.28E+01	9.34E+01
Y1	4.13E+02	1.64E+01	2.38E+01	2.40E+02	2.00E+01	1.17E+02

Table 4.2: Activity Concentration for the NORMs and their progenies in Bq/kg for the soil taken with 100 cm below ground level

	^{210}Pb	^{238}U	^{228}Th	^{226}Ra	^{228}Ra	^{40}K
B2	5.44E+02	1.49E+01	2.63E+01	2.26E+02	2.27E+01	1.40E+02
C2	2.62E+02	7.12E+00	1.10E+01	1.12E+02	9.42E+00	4.03E+01
Fs	3.05E+02	3.99E+01	3.03E+01	2.05E+02	1.63E+01	3.13E+01
G2	5.73E+02	1.68E+01	1.77E+01	2.01E+02	1.68E+01	1.03E+02
H2	8.67E+02	1.31E+01	1.94E+01	2.09E+02	1.59E+01	4.40E+01
I2	1.13E+03	1.40E+01	2.24E+01	2.30E+02	1.96E+01	1.25E+02
J2	1.31E+03	3.07E+01	4.46E+01	5.32E+02	3.66E+01	1.67E+02
K2	5.32E+02	1.43E+01	2.53E+01	2.18E+02	2.04E+01	1.01E+02
L2	6.16E+02	1.03E+01	3.15E+01	1.74E+02	1.54E+01	1.00E+02
M2	2.87E+02	7.77E+00	1.73E+01	1.72E+02	1.66E+01	8.96E+01
N2	1.40E+03	1.00E+01	3.91E+01	3.83E+02	2.14E+01	1.38E+02
O2	1.55E+03	1.50E+01	3.84E+01	3.10E+02	1.92E+01	1.49E+02
P2	7.30E+02	1.16E+01	1.79E+01	1.68E+02	1.62E+01	1.24E+02
Q2	5.54E+02	1.00E+01	1.92E+01	1.71E+02	1.47E+01	7.72E+01
R 2	4.34E+02	7.81E+00	1.60E+01	1.56E+02	1.37E+01	9.29E+01
S2	6.21E+02	3.99E+01	3.33E+01	2.01E+02	2.54E+01	1.52E+02
U2	6.18E+02	1.44E+01	2.01E+01	2.72E+02	1.84E+01	5.99E+01
W2	1.29E+03	1.83E+01	3.50E+01	3.52E+02	1.69E+01	8.49E+01
X2	4.20E+02	4.98E+00	1.90E+01	1.92E+02	1.49E+01	7.73E+01

NB: Tables 4.1 and 4.2 extracted from Annexure 2, errors deliberately omitted due to space and for errors see annexure 2

The graph, Figure 4.2, shows a plot of activity concentrations for each radionuclide plotted against each sampling point. The different radionuclides are classified by different colours.

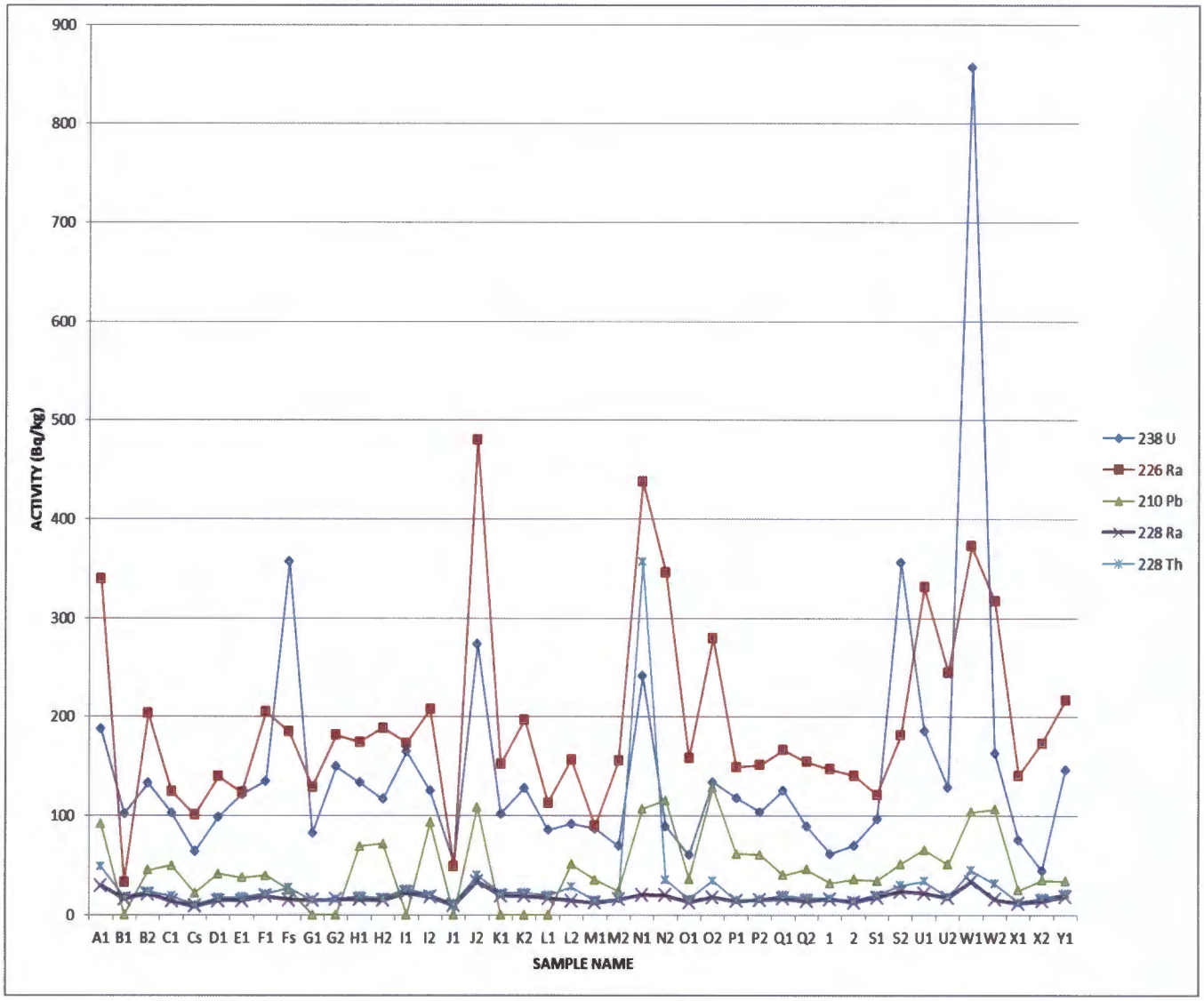

Figure 4.2: Activity concentrations in Bq/kg for each sampling point from Princess Mine Dump

Sampling points W and N taken from opposite ends of the dump but located on the sloping sides of the dump have relatively high values of up to 1290 Bq/kg (point W) and 1400 Bq/kg (point N), compared to the averages 195 Bq/kg and 149 Bq/kg, respectively. At the points W and N, almost all the radionuclides have highier activity concentrations than the average concentrations of the different radionuclides for the whole dump.

Table 4.3: Average activity concentrations for the radionuclides in the topsoil, bottom soil and the whole mine dump

	^{210}Pb	^{238}U	^{228}Th	^{226}Ra	^{228}Ra	^{40}K
Top soil	5.34E+02	1.65E+01	2.31E+01	1.89E+02	1.82E+01	9.43E+01
Bottom soil	7.39E+02	1.58E+01	2.55E+01	2.36E+02	1.84E+01	9.98E+01
overall	7.39E+02	1.61E+01	2.55E+01	2.36E+02	1.84E+01	9.98E+01

In table 4.3, the average activity concentrations for each radionuclide analysed from Princess Mine dump are presented. The average activity concentrations for the whole dump were 639.8 ± 94 Bq/kg, 16.14 ± 32 Bq/kg, 24.89 ± 1.3 Bq/kg, 214.49 ± 37 Bq/kg, 18.61 ± 1.2 Bq/kg, and 97.39 ± 8.5 Bq/kg for ^{210}Pb, ^{238}U, ^{232}Th, ^{226}Ra, ^{228}Ra and ^{40}K, respectively. The world averages by UNSCEAR, 2008 are 33 Bq/kg, 35 Bq/kg, 45 Bq/kg and 412 Bq/kg for for ^{238}U, ^{226}Ra, ^{232}Th and ^{40}K, respectively (UNSCEAR, 2008). The calculated average activity concentrations for the NORMs in the dump are lower than the world averages given by UNSCEAR, except for ^{226}Ra. However when taking a closer look at these averages, it can be seen that the bottom soil is more radioactive compared to the topsoil, except for only ^{238}U, where the opposite is true.

4.3 Investigation of mobility of radionuclides

The mobility of the radionuclides or the movement with depth was investigated by taking the ratios of the activity concentrations of the radionuclides in the top soil to bottom soil. The results are plotted in figure 4.3.

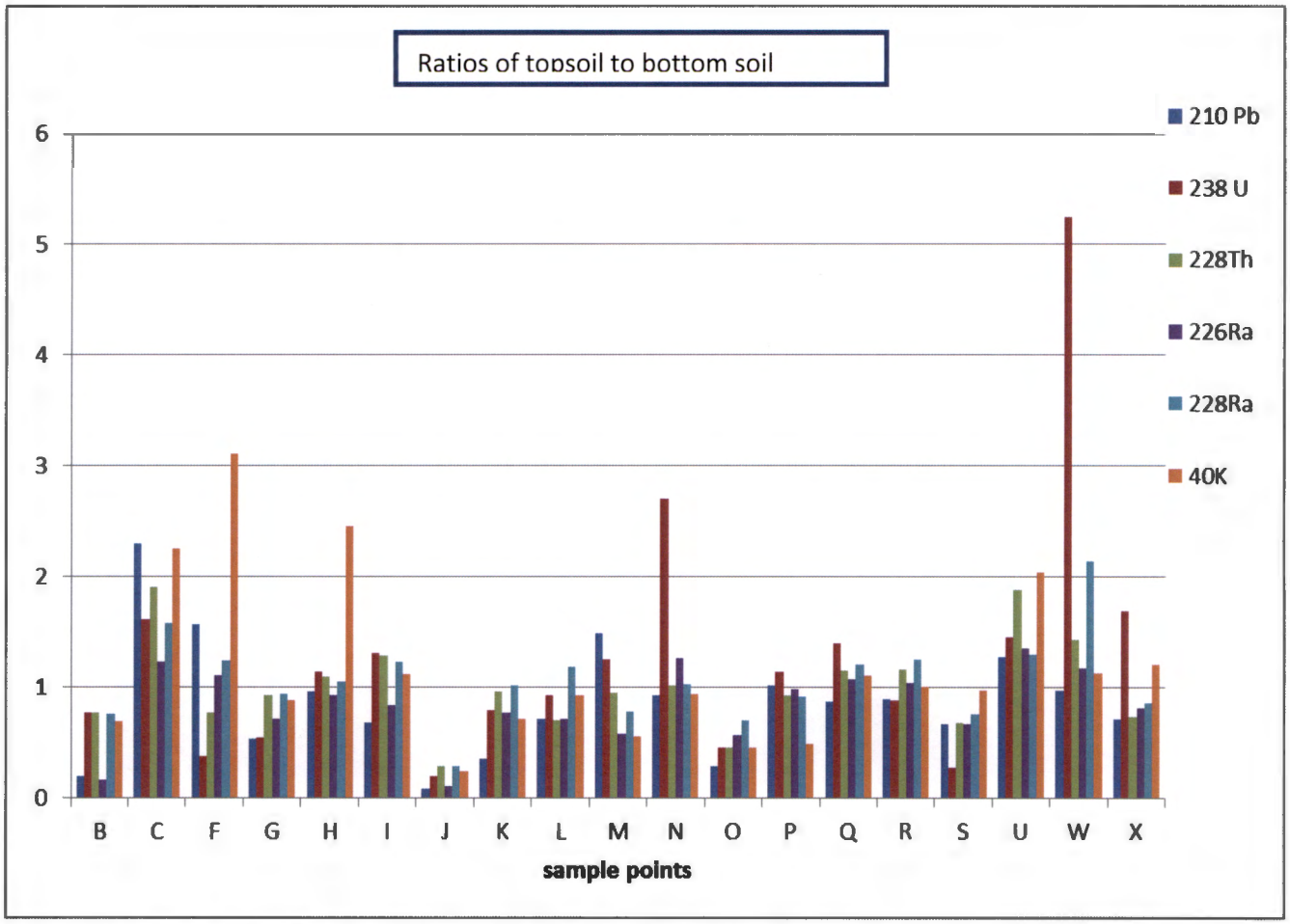

Figure 4.3: Ratios of the top soil to bottom soil for the different radionuclides.

Figure 4.3 above shows the ratios of the top to bottom soil for each of the radionuclides analysed. The ratios as shown in figure 4.3 show no uniformity in the activity concentrations. Sampling points G, H, L, N, P, R, and X show no difference in the concentrations of the radionuclides in the top and the bottom soil. All sampling points with ratios that are less than one (B, J, O, and S) show that the top soil concentrations were lower than the bottom soil and the rest of the points show no trend as they have different ratios for different radionuclides. From figure 4.3 therefore since there is no clear trend that is followed and so it can be concluded that there is no systematic leaching of the nuclides from the topsoil to the bottom soil.

4.4 Determination of radium equivalent and absorbed dose

Equation 14 and 13 were used to calculate the absorbed dos rate due to the presence of the dump and the radium equivalent. Figure 4.4 shows a plot for the absorbed dose due to the presence of the mine dump in nGy/h which was calculated

using equation 14. The values for the absorbed dose ranged from 47.4 to 467 nGy/h and the average was 94.6 nGy/h. Further, what can be noted from the graph is that the point U, had a very high value compared to the others which were above 400 nGy/h.

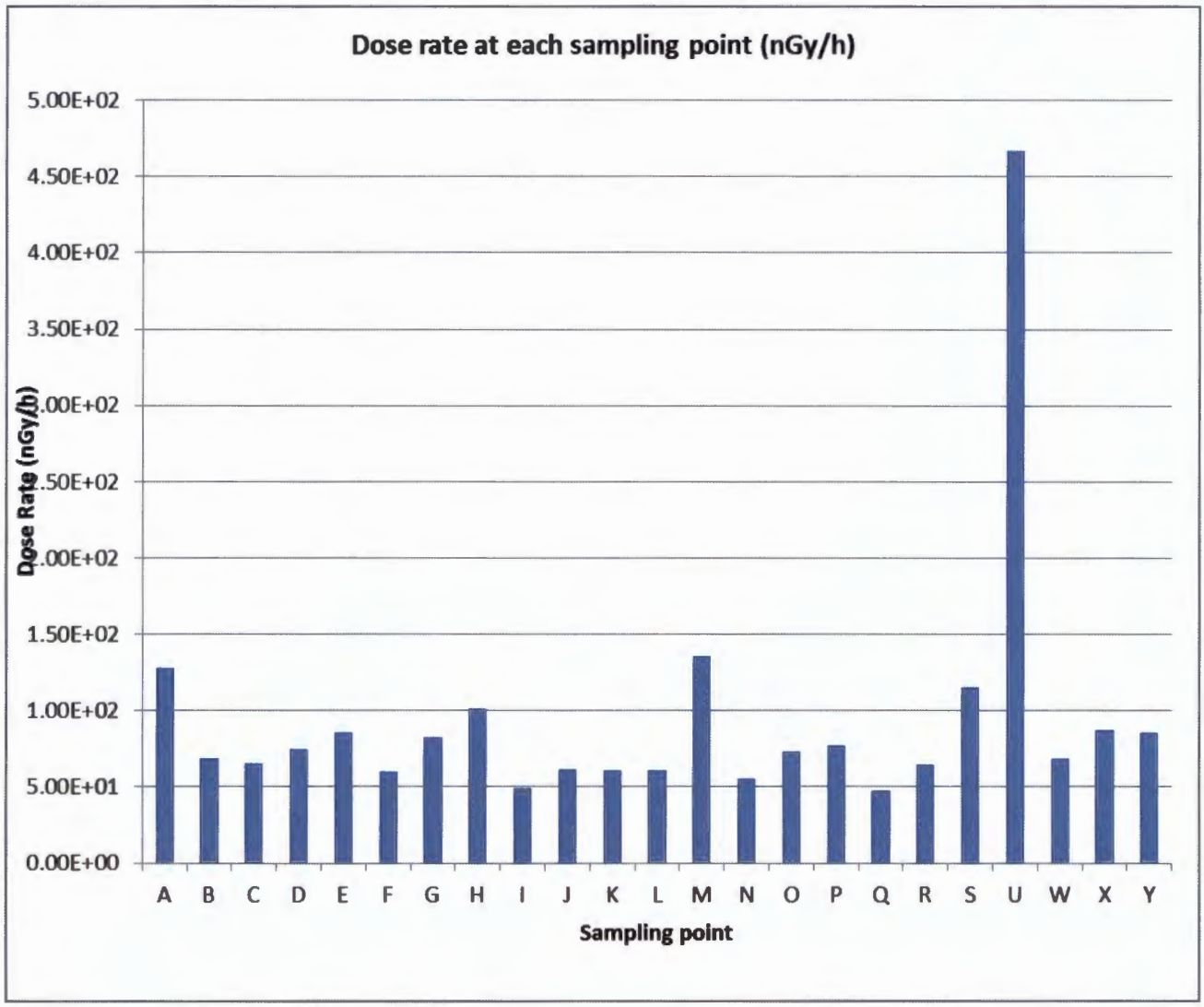

Figure 4.4: Dose rate against each sampling point

Equation 13 was also used to calculate the radium equivalent. The values for the radium equivalent ranged from 105 to 413 Bq/kg as shown in figure 4.5. The radium equivalent is a measurement parameter for estimation of radiation exposure. It comes from the assumption that 370 Bq/kg ^{226}Ra, 259 Bq/kg ^{232}Th or 4810 Bq/kg ^{40}K produce the same gamma dose rate. The calculated world average radium equivalent according to UNSCEAR, 2008 is 370 Bq/kg (Momcilovic et al, 2010).

The hazard index was also calculated using equation 18 and the average was 0.68. This value is quite high compared to many studies that have been done in other parts of the world. A perfect example is the Haryana mining regions in India (Kensal et al, 2012) that is below unity which is the limit given by the UNSCEAR, 2000.

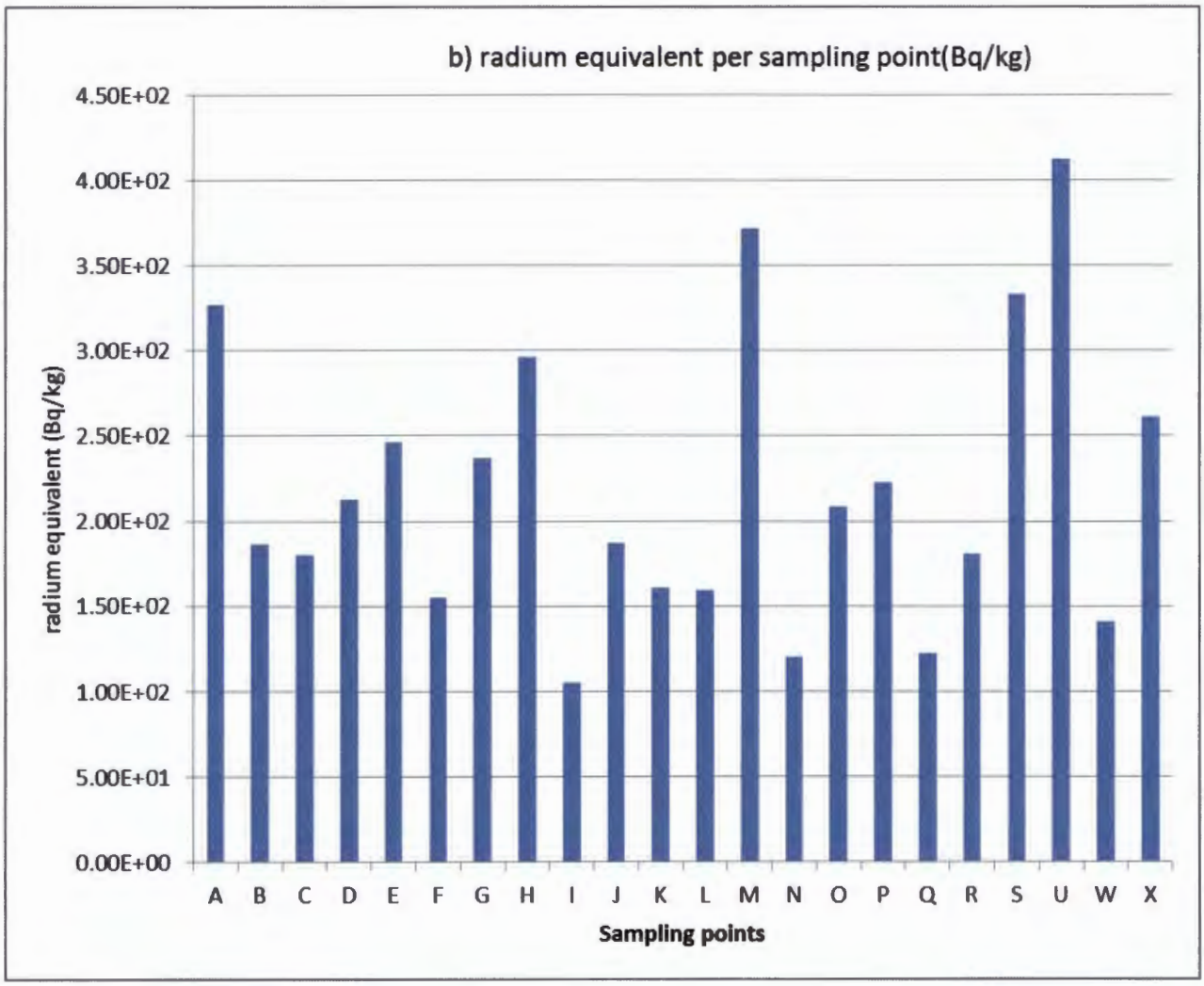

Figure 4.5: The radium equivalent against each sampling point

4.5 Estimation of transfer to dust and calculation of AEDE

Also calculated was the estimated internal absorbed inhalation from dust particles. These were calculated using the international standards, for the yearly intake from of dust by humans and the average dust concentration of the Gauteng region given in the standard tables given by the IAEA series and the National Nuclear Regulatory guide (NNR-RG2). Table 4.4 below shows the calculated concentrations of the

different radionuclides in the soil, using the estimated dust concentration in the Gauteng region, which is 50μg/m^3. This was calculated from the measured activity concentrations of the gamma emitting radionuclides and assuming that the dust concentration is 50μg/m^3. Therefore the concentrations in the table below are in μBq/m^3. These values or concentrations in table 4.4 are used to estimate the internal dose as they cover the approximate amounts of radionuclides that can be taken by dust at standard conditions.

Table 4.4: The calculated activity concentrations from dust concentration of 50μg/cm^3

sample	^{238}U	^{226}Ra	^{228}Ra	^{40}K
A	1.05E+01	1.88E+01	1.59E+00	5.86E+00
B	5.74E+00	1.81E+00	8.60E-01	4.86E+00
C	5.53E+00	6.90E+00	7.47E-01	4.53E+00
D	6.80E+00	7.73E+00	7.70E-01	2.14E+00
E	7.54E+00	6.84E+00	7.63E-01	6.96E+00
F	4.60E+00	1.14E+01	1.01E+00	4.87E+00
G	7.47E+00	7.13E+00	7.92E-01	4.56E+00
H	9.21E+00	9.65E+00	8.33E-01	5.41E+00
I	2.93E+00	9.62E+00	1.20E+00	7.01E+00
J	5.71E+00	2.67E+00	5.22E-01	2.03E+00
K	4.79E+00	8.42E+00	1.04E+00	3.59E+00
L	4.86E+00	6.25E+00	9.09E-01	4.64E+00
M	1.35E+01	4.97E+00	6.50E-01	2.47E+00
N	3.37E+00	2.42E+01	1.10E+00	6.48E+00
O	6.60E+00	8.76E+00	6.75E-01	3.37E+00
P	7.02E+00	8.26E+00	7.46E-01	3.05E+00
Q	3.44E+00	9.22E+00	8.83E-01	4.29E+00
R	5.39E+00	8.14E+00	8.61E-01	4.67E+00
S	1.04E+01	6.73E+00	9.62E-01	7.40E+00
U	4.80E+01	1.84E+01	1.19E+00	6.12E+00
W	4.21E+00	2.07E+01	1.81E+00	4.79E+00
X	8.20E+00	7.79E+00	6.38E-01	4.67E+00
Y	7.32E+00	1.20E+01	1.00E+00	5.86E+00

Annexure 4 shows a table that was constructed by the IAEA for the annual uptakes of radionuclides dose in Sv/Bq for different age groups. The total inhaled dose from dust was calculated using the activity concentrations for each radionuclide in the air (given in table 4.4) and the standard inhalation rates given by the IAEA series (annexure 4). These were used to calculate the yearly dose from internal radiation using equation 15 and the resulting table from the calculations yielded the annual effective dose equivalent (AEDE) in mSv/a from each radionuclide which is hown in table 4.5.

Table 4.5 Annual effective dose equivalent for different age groups

Nuclide/age	< 1 a	1 -2 a	2-7 a	7-12 a	12-17a	>17 a
^{238}U	8.97E-04	7.73E-04	8.01E-04	9.43E-04	1.23E-03	1.11E-03
^{234}Th	1.27E-06	9.59E-07	8.51E-07	1.04E-06	1.29E-06	1.08E-06
^{234}U	1.02E-03	8.97E-04	9.51E-04	1.13E-03	1.41E-03	1.32E-03
^{230}Th	6.50E-03	6.19E-03	7.01E-03	1.04E-02	1.40E-02	1.40E-02
^{226}Ra	1.23E-03	1.05E-03	1.12E-03	1.33E-03	1.66E-03	1.56E-03
^{214}Pb	2.50E-06	1.81E-06	1.64E-06	2.32E-06	2.48E-06	2.46E-06
^{214}Bi	3.15E-06	2.21E-06	1.82E-06	2.43E-06	2.82E-06	2.29E-06
^{210}Pb	6.52E-04	6.52E-04	6.54E-04	7.95E-04	9.77E-04	8.36E-04
^{210}Bi	1.41E-05	1.09E-05	1.11E-05	1.44E-05	1.82E-05	1.52E-05
^{210}Po	6.52E-04	5.07E-04	5.04E-04	6.51E-04	8.54E-04	7.05E-04
^{232}Th	3.31E-05	3.16E-05	3.72E-05	5.69E-05	7.88E-05	7.15E-51
^{228}Ra	7.04E-06	6.90E-06	7.45E-06	8.76E-06	1.05E-05	1.04E-05
^{228}Ac	2.59E-08	2.30E-08	2.26E-08	2.50E-08	1.91E-08	1.63E-08
^{228}Th	2.59E-05	2.16E-05	1.93E-05	2.41E-05	3.09E-05	2.60E-05
^{224}Ra	1.72E-06	1.32E-06	1.37E-06	1.93E-06	2.76E-06	2.21E-06
^{212}Pb	9.63E-08	7.19E-08	7.68E-08	1.09E-07	1.58E-07	1.24E-07
^{212}Bi	2.30E-08	1.58E-08	1.40E-08	1.93E-08	2.50E-08	2.02E-08

4.5 Discussion

The results, as they can be shown in the previous chapter, show that there are radionuclides present in the mine tailing as expected from the literature review. There is a number of naturally occurring radionuclides as shown in the figure 4.1. The NORMS available were from the uranium series and the thorium series. Even though, due to the limitations of the instruments that was used, which are poor resolution of peaks in the lower energies in the HPGe and also the inability of the ICP-MS to separate the different isotopes being measured, not all the radionuclides

were identified, most of the known gamma emitting radionuclides were identified, using their abundant gamma lines.

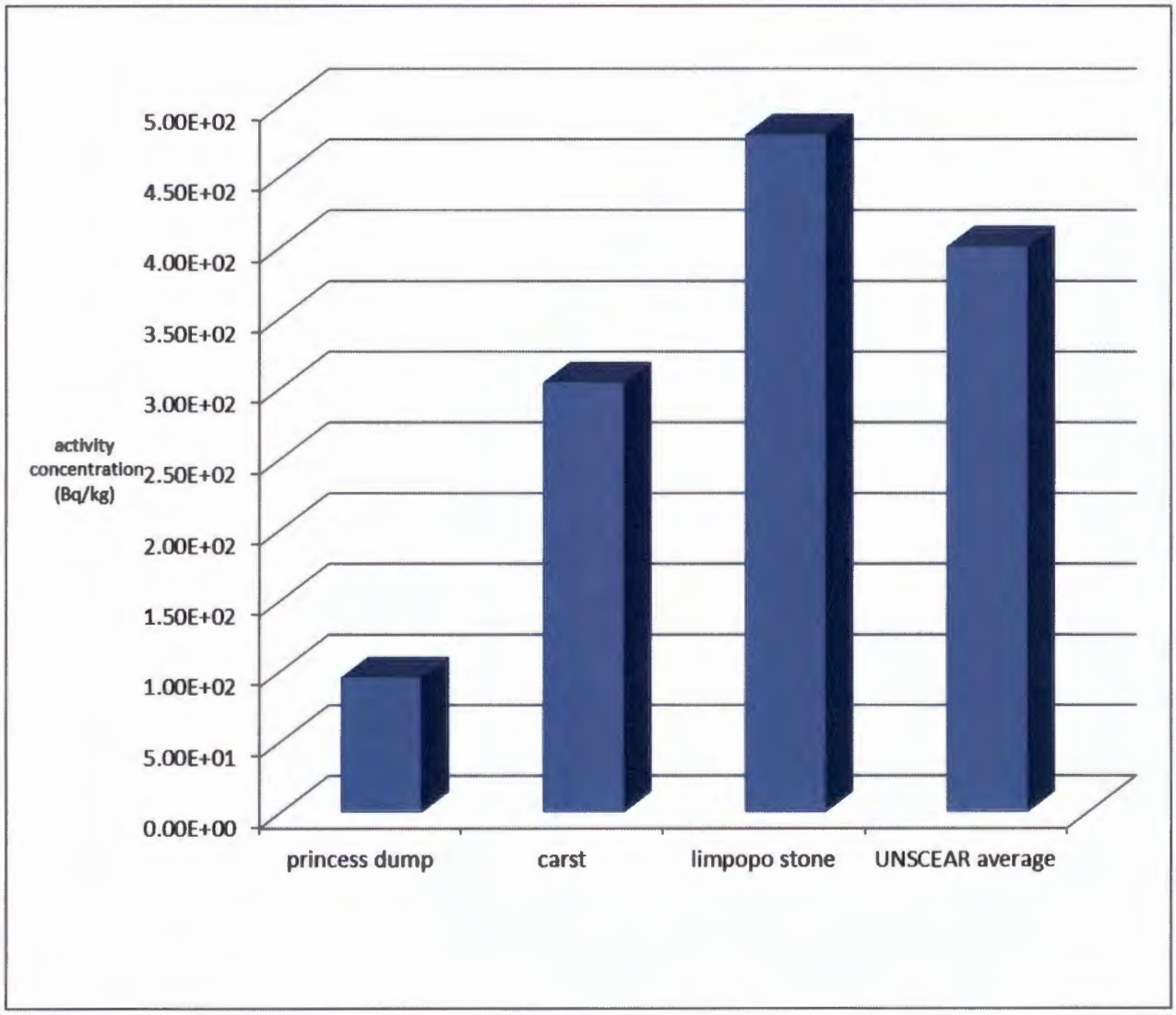

Figure 5.1: Average activity concentration for ^{40}K in Bq/kg for princess dump and two other places and also the UNSCEAR world average

The spectra of the soil sample also show a difference in the ratio of the other radionuclides to ^{40}K. This was confirmed using samples that were taken from the university soil and also some soil that was taken from a remote area, in the Limpopo province. These samples also backed by a literature search show that ^{40}K, usually has a higher activity compared to the other radionuclides. This therefore means that there is a difference in the soil samples from the mine dump as they show a reduction in the activity concentration of ^{40}K compared to other known areas, and this may be an area for further research. Figure 5.1 shows the comparison of the average activity concentrations of ^{40}K for three places and the world average.

The average activity concentrations for the top soil, bottom soil and the overall averages for each radionuclide that was analysed are shown in table 4.3. These results show that generally the bottom soil is more radioactive than the topsoil except for ^{238}U. Possible reasons for the observed trends can be leaching of the radionuclides into lower depths and erosion of the topsoil. The average concentrations of the radionuclides are lower than the world averages given by UNSCEAR, 2008 except for ^{226}Ra. The overall averages for ^{210}Pb, ^{238}U, ^{232}Th, ^{226}Ra, ^{228}Ra and ^{40}K are 639.8 ± 94 Bq/kg, 16.14 ± 3.2 Bq/kg, 24.89 ± 1.3 Bq/kg, 214.49 ± 37 Bq/kg, 18.61 ± 1.2 Bq/kg, and 97.39 ± 8.5 Bq/kg respectively. These are lower than the world averages given by UNSCEAR which are are 33 Bq/kg, 35 Bq/kg, 45 Bq/kg and 412 Bq/kg for for ^{238}U, ^{226}Ra, ^{232}Th and ^{40}K respectively.

The rate of leaching or mobility of the radionuclides in the mine dump is very minimal and non-uniform. This is shown by the non-uniformity of the trends in the topsoil and the bottom soil of the mine dump. There is no any significant trend that can give information on whether radionuclides do move or leach into the soil or are carried by water into the soil. Here there may be many reasons for this like the mine dump is old and the mobile radionuclides moved a long time ago and there is no longer any movement or it is just because they don't move at all. This also maybe a pathway for further research, involving the deep digging to find out whether there are some radionuclides that were leached deep into the ground.

The radiation exposure and the safety of the environment are not very compromised by the presence of the mine dump. Though it is tampering with the landscape it posed no health risks to the environment around it. This is evident from the calculated Ra equivalent and the annual effective dose equivalent which are, 118 nGy/h and 223 Bk/kg, respectively and are well below the limits by UNSCEAR, 2000, and the ICRP. Also the hazard index is 0.68 which also meant the mine dump isn't a hazard to the adjacent community. This means therefore that the sand from the mine dump can be used for everyday activities and also the mine dump poses no harm to humanity.

Comparisons were done using the results with soil that was taken from other places which are not from the Princess Mine Dump. This showed that the soil from Princess Mine Dump was more radioactive than the other two samples. The two respective soil samples were from CARST in the North-West University and from a stone taken from Thohoyandou, Limpopo province.

Lastly, transfer of radionuclides to dust was calculated, assuming the dust concentration of the surrounding areas was equal to the dust concentration of the whole country. This estimate also shows that the mine dump poses no harm as the average AEDE calculated was 0.087mSv/yr, which is lower than the limit set by UNSCEAR, 2000. Figure 5.2 shows a bar chart that compares the annual effective dose calculated for the three different places including the current study, using the assumption that the dust concentration is 50μ/cm^3. From this chart Princess Mine Dump has a higher average compared to the other two places.

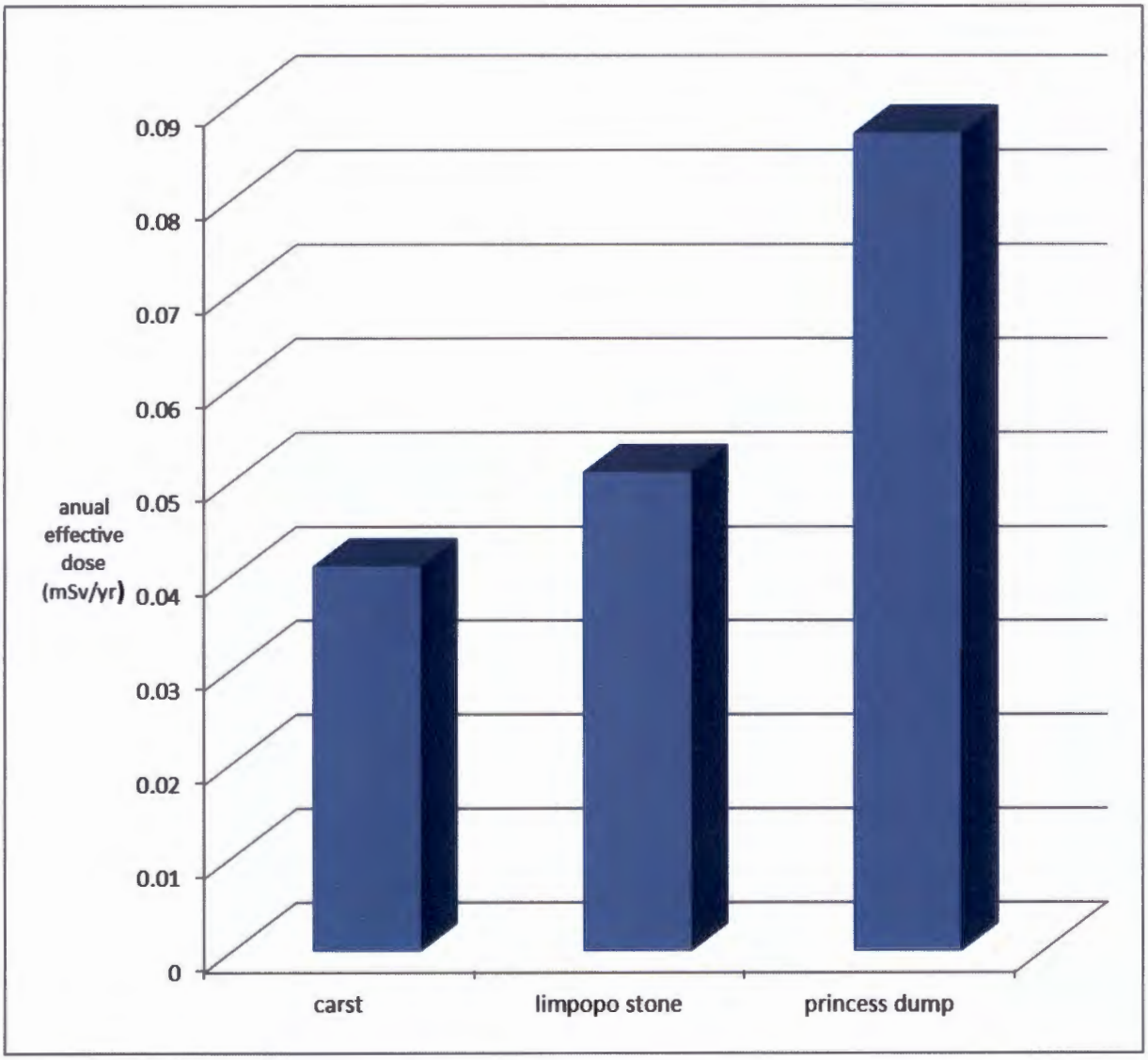

Figure 5.2: A comparison between the annual effective dose from Princess Mine Dump with two other places

Table 5.1 shows the dose rates from selected mining areas around the world, and these are compared to the finding of the current study. The observation from the results is that there is no significant difference in the dose from Princess Mine Dump and the mining areas in other places around the world.

Table 5.1: Gamma dose rates in nGy/h and annual effective dose rates in mSv/yr from selected mining areas around the world (Momcilovic et al, 2010)

Country	region	gamma dose rate(nGy/h)	annual effective dose (mSv/yr)	
Hungary	Kovagoszolos	95 -252	0.12 - 0.31	
	Cserkut	78 - 123	0.09 - 0.15	
Kyrgyzstan	Mailulu Saa	148	0.18	
India	Musabani	233	0.28	
	Phanthagora	429	0.52	
	Badia	263	0.32	
	Bhatin	3155	3.86	
Australia	Naberlek	125 - 300	0.15 - 0.37	
Serbia	Stara Platnnina	216 - 422	0.06 - 0.27	
South Africa	Rooderpoort	47 - 467	0.06 - 0.57	(this study)

CHAPTER 5: CONCLUSIONS AND FUTURE WORK

5.1 Conclusions

The natural radioactivity of the soil samples that were taken from Princess Mine Dump was evaluated using a High Purity germanium detector. The results showed that primordial radionuclides from the Thorium, Uranium, and actinium series and also Potasium-40 were contained in all the samples.

The activity concentrations of the different radionuclides were analyzed and the averages were 16.1 ± 3.2 Bq/kg, 24.9 ± 1.3 Bq/kg, 214.5 ± 37 Bq/kg, and 97.39 ± 8.5 Bq/kg for ^{238}U, ^{232}Th, ^{226}Ra, and ^{40}K, respectively. The world averages by UNSCEAR, 2008 are 33 Bq/kg, 35 Bq/kg, 45 Bq/kg and 412 Bq/kg for for ^{238}U, ^{226}Ra, ^{232}Th and ^{40}K respectively (UNSCEAR, 2008). However a concern can be from the fact that some of the activities in some sampling points were way above the world averages given by the regulatory body mentioned above.

The ratios of the activity concentrations for topsoil and bottom soil were calculated to determine to determine vertical mobility of the radionuclide. No conclusion can be drawn from these results because they show no uniformity, also the inhomogeneity of the radionuclide distribution initially.

The radium equivalent and the absorbed dose at one metre above the dump were calculated. The average radium equivalent was 223 Bq/kg which shows that ^{226}Ra poses no health threats to the humans as the values are below world averages which are 370 Bq/kg. This is in spite of the dose rate due to the presence of the Dump 118 nGy/h, which is almost two times higher than the world average which is 58 nGy/h according to UNSCEAR 2008.

The estimated transfer of radionuclides to dust was determined and then the annual effective dose equivalent was calculated and found to be below unity as required by the UNSCEAR limits.

5.2 Future work

The results of the study in general show that the Mine Dump is different from the natural environment but also indicate that it poses no health hazard. The results have some loopholes though:

Proper leaching studies of the movement of the radionuclides needs to be done. They also present a necessity for an integrated approach for radiation impact assessment on specific communities as some sampling points had some alarming figures.

A follow-up study on why the efficiency curve is different from the normal one as seen in other literature sources, and also the factors affecting the shape of the curve.

Lastly, dust sampling should be done to reduce the uncertainty that is a result of the estimations.

REFERENCES

Ahmed N. K, El-Arabi, A G M, 2005, Natural radioactivity in farm soil and phosphate fertilizer and its environmental implications in Qena governorate, Upper Egypt, *Journal of Environmental Radioactivity*. 84:51-64

Allen B., Marcu L., Bezak E., 2012, Biomedical physics in radiotheraphy for cancer, CSIRO Publishing Collingwood

AMS samplers, n.d. *The world's finest sampling equipment*, http://www.ams-samplers.com/category.cfm?CNum=6 viewed 27 September 2014

Ballare C. L., Scopel A. L., Sanchez R. A., 2000, Photocontrol of sterm elongation in plant neighbourhoods: effects of photon fluence rate under natural conditions of radiation, *Journal of Plant cell and Environment*. 14:p57-65

Battacharyya D. K., 1998, Issues in the disposal of waste containing NORM, *Journal of applied Radiation and Isotopes* 49: 215-226.

Bode P., 1998, Detectors of radiation, Delft University of technology, Netherlands

Cheng H., Edwart R. L., Hoff J, Gallup C. D., Richards D. A., Asmeron Y., 2000, The half-lives of Uranium-234 and Thorium-230, *Journal of chemical geology*, 169:17-33

Ciffroy P., Durrieu G., and Garnier J., 2009, Probabilistic distribution coefficients (K_ds) in freshwater for radioisotopes of Ag, Ba, Be, Ce, Co, Cs, I, Mn, Pu, Ra, SB, Sr, and Th- implications for uncertainty analysis models simulating the transport of radionuclides in rivers, *Journal of environmental radiation*, 100:766-722

Daraban L., Iancu D. and Nita D., 2012, Efficiency calibration in gamma spectrometry by using ^{232}Th series radionuclides, *Romanian journal of physics*:58: 99-107.

Davies, T.C. and Mundalamo, H.R., 2010, Environmental health impacts of dispersed mineralization in South Africa, *Journal of African Earth Sciences,* 58: 652 - 666.

Eschenauer M., Wirowski R., Marcus D. and von Brentano P., 1994, Resolution enhancement of gamma-spectroscopy data from neutron-damaged coaxial n-type HPGe-detectors, *Nuclear Instruments and Methods in Physics Research*.340: 364-370

Fayazi M., 2005, Report on the water quality survey around the Princess Mine Dump and its negative effects on the water resources (both surface water and ground water).

Gopal B. S., 2010, Physics and radiobiology of nuclear medicine, Springer science and Business media, New York

Greening J R., 1985, Fundamentals of dosimetry, second edition, CRC Press, New York (Taylor and francis group)

Gross C. T., 1999, Developments in ICP-MS: Electrochemically Modulated Liquid Chromatography for the Clean-up of ICP-MS Blanks and Reduction of Matrix Effects by Flow Injection ICP-MS, PhD thesis, Department of Analytical Chemistry, Iowa state university

Harald M., 1992, Multivariate calibration, John Wiley and Sons, New York

Harvey B. G., 1969, Introduction to Nuclear Physics and Chemistry (2nd edition), Springer science and business media, New Jersey, Prentice town

Hayumbu P., Mulenga S., Nomai M., Mulenga P., Katebe R., Shaba P., Chunga T., Inambao D., Mangala F., Tembo P., Malama Y., 2004, Status of radon dosimetry in Zambian underground mines, Naturally occurring radioactive materials (NORM IV), International conference Proceedings held in Szczyrk, Poland, 17–21 May 2004

Hobbie R. K., and Roth B. J., 2007, Intermediate Physics for medicine and biology, Springer Science and Business, Media, New York,

Hossain M. K., Hossain S. M., Azim R., Mease A. M. H., 2010, Assessment of radiological contamination of soils due to ship breaking using HPGe gamma-ray spectrometry system. *Journal of environmental protection*, 1:10-14.

http://www.epa.gov/rpdweb00/understand/equilibrium.html, retrieved 13 October 2013

IAEA, Modelling the environmental transport of tritium in the vicinity of long-term atmospheric and sub-surface sources, IAEA-BIOMASS-3, IAEA, Vienna (2003).

IAEA, 2007, Modelling the transfer of radionuclides from Naturally Occurring Radioactive material: Report of the NORM working Group of (Environmental Modeling for Radition safety) theme 3

ICRP Publication 92: Relative Biological effectiveness Quality factor and Radiation weighting factor(wR), Jack Velentin, Sarge publication, New York, 2003.

Irin Humanitarian news, 2012, South Africa paying the price of gold, http://www.irinnafrica.org/report/76780/south-africa/south-africa-paying-the-price-of-gold/ , retrieved 22 September 2013

Kansal S, Mehra R, Singh N P, Badhan K and Sonkawade R G, 2010, analysis and assessment of radiological risk in soil samples of Hisar district of Haryana, India, *Indian journal of pure and applied physics*.48:512-515

Karahan G, Bayulken A, 2000, Assessment of gamma dose rates around Istanbul,(Turkey), *Journal of Environmental Radioactivity,* 47: 213-221

Konya J and Nagy N, 2012, Nuclear and radiochemistry, Elsevier Inc, London

Krane K. S., 1998, Introductory nuclear physics, John Wiley and sons, New York

Kotz J. C., Treichel P. M. and Townsend J, 2009, Chemistry and chemical reactivity Cengage Learning, Belmount

Lutz G, 2001, Semiconductor radiation detectors, springer-Verlag Berlin Heidelberg, New York

Mangset W. E. and Sheyin A. T., 2009, Measurement of radionuclides in processed mine tailings in jos, plateau state. *Bareyo journal of pure and applied sciences*, 2:56-60

Modisane T. J., 2005, Correlations between natural radioactive concentrations in soils and vine growth, MSc thesis, Centre for Applied Radiation Science and Technology, North-West University (Mafikeng campus)

Monte L., 2010, Modelling multiple dispersion of radionuclides through the environment, *Journal of environmental radioactivity*, 101:134-139

Musicale M. R., Anoka O. C. and Balogun F. A., 2011, Radioactivity Measurements of the Jos Tin Mine Tailing in Northern Nigeria, *Archives of Physics Research*, 2:80-86

Ngigi Samuel M., 2009, 'Establishing effective, appropriate and applicable technologies in treating contaminated surface water as part of a rehabilitation strategy for the princess dump in Roodepoort, west of Johannesburg', MSc, department of environmental sicences, University Of Witwatersrand

NNR annual full status report, 2008, http://www.nnr.co.za/wp-content/uploads/2012/05/2007-2008-Annual-Report.pdf , retrieved 30 October 2013

NNR regulatory guide, Assessment of radiation hazards to members of the public from norm activities, 2008, RG002

Nour K., Ahmed, Abdel., Mohamed E., 2005, Natural radioactivity in farm soil and phosphate fertilizer and its environmental implications in Qenagovernorate, Upper Egypt, *and Journal of Environmental Radioactivity*: 84:51-64.

Olley J. M., Murray A., Roberts R. G., 1996, The effects of disequilibria in the uranium and thorium decay chains on burial dose rates in fluvial sediments, *Quaternary Science Reviews*, 15: 751-760,

Ozawa A., 2004, Measurement of reaction cross-section and determination of nucleon matter density distributions, *Hadrons in world physics*, 244: 301-321

OGP, 2008, Guidelines for the management of Naturally Occurring Radioactive Material (NORM) in the oil & gas industry Report No: 412 September 2008

Poenari D. N., Ivascu M. and Samdulescu A., 1979, Alpha decay a fission-like process, *Journal of physics G: Nuclear physics*, 5:L165

Robins M., 2004, Closure of tailings facilities: Current practice review and guidelines for success, Msc Thesis, Faculty of Engineering, University of the Witwatersrand (Civil Engineering).

Santawamaitre T., 2012, , An Evaluation of the Level of Naturally Occurring Radioactive Materials in Soil samples along the Chao Phraya River Basin, PhD thesis, Department of environmental physics, University of Surey.

Srivastava B. B., 2006, Nuclear Physics, Rastogi publications, New Delhi

Skubacz K., and Mielnikow A., 2004, measurement of short lived radon daughters in polish mines. Naturally occurring radioactive materials (NORM IV), International corference Proceedings held in Szczyrk, Poland, 17–21 May 2004

Sima O., Arnold D., and Dovlete C., 2001, GESPECO: a versatile tool in gamma spectroscopy, *Journal of Radioanalytical and Nuclear Chemistry*, 248:359-364

Smith K., 1997, Constructed Wetlands for Treating Acid Mine Drainage, http://conservancy.umn.edu/bitstream/58868/1/2.7.Smith.pdf , retrived 15 august 2013

Smith G. and Baxter M. S., 2007, Radioactivity in the terrestrial environment, Elsevier LTD, Netherlands end Inc

Speelman W. J., Lindsay R., Newman R.T., De Meijer R.J., 2005, Radon generation and transport in and around a goldmine tailings dam in South Africa

Sroor A, El Bahi S. M., Ahmed F., Abdel-Haleem A. S., 2001, Natural radioactivity and radonexhalation rate of soil in southern Egypt, *Journal of applied radiation and Isotopes*, 55: 873-879

Stabin M. G., 2007, radiation protection and dosimentry: An introduction to health physics, springer science and business media LCC, New York.

The Shielding of Radiographic Facilities at Diagnostic facilities, Shielding Design for Diagnostic X-ray rooms Draft of June 1999. http://www.dundee.ac.uk/medphys/documents/draftJune99t.pdf, retrieved 12 March 2014

UNSCEAR, exposures from natural radiation sources with Detailed References, ANNEX B, I (2000) 1-74.

Van der Graaf E. R., Koomans R. L., Limburg J. and Vriers K., 2007, In situ radiometric mapping as a proxy of sediment contamination: Assesment of the underlying geochemical and physical principles, *Journal of applied radiation and isotopes,* 65: 619-633.

Varshini P., Sophie S. and Alice R., 2014, Gamma ray shielding http://scipp.ucsc.edu/outreach/HS_Interns/2013interns/Gamma%20Ray%20Detection.pdf, retrieved 15 March

Venter Zel, 2005, Court sets deadline for pollution clean-up, IOL-news, http://www.iol.co.za/news/south-africa/court-sets-deadline-for-pollution-clean-up-1.300057#.Uw3yVlWwOoU

Verplancke J., 1992, Low level gamma spectroscopy: low, lower, lowest, *Nuclear Instruments and Methods in Physics Research Section A: Accelerators, Spectrometers, Detectors and Associated Equipment*, 312: 174–182

Wendel G., 1998, Radioactivity of mines and water - sources and mechanisms. *South African journal of mining and metallurgy*.

Winde F., and de Villiers A., 2002, The extent of uranium concentration from tailing dams in the Witwatersrand gold mining area, *Journal of uranium in the aquatic environment*, 24 : 889-898

Winde F., 2010, Uranium pollution of the Wonderfonteinspruit, 1997-2008 Part 1: Uranium toxicity, regional background and mining-related sources of uranium pollution, 36: 239-256

Wigner E., 2004, Detectors of radiation, A course on Reactor Physics Experiments, Department of Nuclear Physics and Technology, Slovak University of Technology, Bratislava, Slovakia.
http://www.reak.bme.hu/Wigner_Course/2004/WignerManuals/Bratislava/detectors.pdf, retrieved 2 July 2013

Wilbur S., Proper W., Yamada N. and Sugiyama N., 2008, Direct Analysis of Undiluted Soil Digests Using the Agilent High Matrix Introduction, Accessory with the 7500cx ICP-MS, Agilent Technologies, Inc,.

Yager T R, 2007, the mineral industry of South Africa, 2005 Minerals yearbook

Yu P. and Cardona M., 2010, Fundamentals of Semiconductors: Physics and Materials Properties, Springer Science and business media, berlin Heidelberg

Appendices

Annexure1: Norm decay series

a) Table 1 ^{238}U decay series

Nuclide	Half-life	Major Gamma Radiation Energies (MeV) and Intensities
^{238}U ↓ α	4.5×10^9 a	0.04955 (22.46%) 0.1135 (0.013%)
^{234}Th ↓ β	24.1 d	0.0924 (16.2%)
^{234m}Pa (99.86%) ↓ β	1.18 min	0.0435 (1.42%) 1.001 (0.856%)
^{234}U ↓ α	2.38×10^5 a	0.0532 (28.7%)
^{230}Th ↓ α	7.52×10^4 a	0.068 (0.38%)
^{226}Ra ↓ α	1602 a	0.1862 (5.962%)
^{222}Rn ↓ α	3.825 d	0.511 (0.078%)
^{218}Po ↓ α	3.05 m	0.837 (0.0011%)
^{214}Pb ↓ β	26.8 m	0.2952 (27.3%) 0.3519 (46.96%)
^{214}Bi (99.98%) ↓ β	19.7 m	0.609 (46.4%) 1.1203 (15.14%)
^{214}Po ↓ α	164 μs	0.799 (0.0105%)
^{210}Pb ↓ β	22,3 a	0.047 (80.2%)
^{210}Bi ↓ β	5.02 d	0.305 (0.000084%)
^{210}Po ↓ α	138.3 d	0.803 (0.00124%)
^{206}Pb	stable	

Minor branches omitted

Table 2 ^{235}U decay series (Actinium series)

Nuclide	Half-life	Major Gamma Radiation Energies (MeV) and Intensities
^{235}U ↓ α	7.13×10^8 a	0.144 (13.5%) 0.186 (63.4%)
^{231}Th ↓ β	24.64 h	0.059 (75.1%) 0.084 (23.4%)
^{231}Pa ↓ α	3.43×10^4 a	0.300 (4.25%) 0.303 (2.62%)
^{227}Ac (98.8%) ↓ β	21.8 a	0.0693 (0.0076%)
^{227}Th ↓ α	18.17 d	0.236 (12.6%)
^{223}Ra ↓ α	11.68 d	0.1542 (28.2%) 0.2695 (25.5%)
^{219}Rn ↓ α	3.92 s	0.2712 (13.3%) 0.4018 (7.12%)
^{215}Po ↓ α	1.83 ms	0.4389 (0.06%)
^{211}Pb ↓ β	36.1 m	0.4048 (4.3%) 0.4272 (2.13%) 0.832 (3.6%)
^{211}Bi (98.7%) ↓ α	2.16 m	0.351 (16.16%)
^{207}Tl ↓β	4.79 m	0.8978 (0.269%)
^{207}Pb	stable	

Minor branches omitted

b) Table 3 ^{232}Th decay series

Nuclide	Half-life	Major Gamma Radiation Energies (MeV) and Intensities
^{232}Th	1.39×10^{10} a	0.064 (0.26%)
↓ α		
^{228}Ra	5.75 a	0.0264 (28%)
↓ β		
^{228}Ac	6.13 h	0.0578 (72.5%) 0.338 (11.7%) 0.911 (26.5%)
↓ β		
^{228}Th	1.913 a	0.0844 (26.4%)
↓ α		
^{224}Ra	3.64 d	0.241 (5.26%)
↓ α		
^{220}Rn	55.6 s	0.550 (0.118%)
↓ α		
^{216}Po	0.14 s	0.805 (0.0019%)
↓ α		
^{212}Pb	10.64 h	0.2386 (81.6%) 0.3001 (4.66%)
↓ β		
^{212}Bi → (36%)	60.5 m	0.0399 (26.0%) 0.727 (6.74%)
(64%) ↓ β ↓ α		
	304 ns	No gamma
^{212}Po ↓		
↓ α	3.1 m	0.583 (86.7%) 2.6145 (100%)
^{208}Tl		
↓ ↓ β		
	Stable	
^{208}Pb ←		

Minor branches omitted

Annexure 2

a) **Table 1 showing raw and uncorrected results from the detector**

sample name	Pb210 46.5 keV		U238 92.4 keV		Th228 238 keV		Ra226 351 keV		Ra228 911keV		K40 1460.5 keV		
	A (Bq)	E (Bq)	A (Bq)	E (Bq)	A (Bq)	E (Bq)	A (Bq)	E (Bq)	A (Bq)	E (Bq)	A (Bq)	E (Bq)	Mass of sample
A1	5.88	5.6	12.1	4.1	3.12	0.75	21.9	5.1	1.89	0.62	7.16	2.6	0.27741
B1	0.624	1.2	7.12	2	1.26	0.28	2.28	0.56	1.11	0.38	6.42	2.34	0.30022
B2	2.23	2.9	6.58	1.9	1.17	0.26	10.1	2.4	1.04	0.36	6.56	2.4	0.21333
C1	3.51	3.5	7.23	2.1	1.33	0.301	8.78	2.1	0.974	0.34	6.05	2.1	0.30319
Cs	1.43	2	4.2	1.4	0.652	0.15	6.66	1.6	0.575	0.201	2.52	1.02	0.2841705
D1	2.71	3.3	6.47	1.9	1.12	0.29	9.15	2.2	0.933	0.33	2.66	1.5	0.28201
E1	2.4	2.4	7.81	2.1	1.15	0.26	7.94	1.49	0.907	0.31	8.47	3.9	0.27654
F1	2.7	2.7	9.19	2.5	1.43	0.32	14	3.3	1.28	0.43	6.3	2.6	0.29358
Fs	1.76	2.5	24.9	2.1	1.9	0.47	12.9	3	1.05	0.36	2.07	1.8	0.30027
G1	1.72	2.5	5.61	1.7	1.01	0.23	8.79	2.1	1	0.34	5.9	3	0.29379
G2	3.42	4	10.8	2.9	1.15	0.26	13.1	3.1	1.12	0.38	7.04	2.6	0.3104
H1	4.75	4.6	9.19	2.5	1.31	0.29	12	2.8	1.06	0.36	7.06	5.7	0.29619
H2	5.4	5.2	8.79	2.4	1.31	0.29	14.2	3.3	1.11	0.38	3.14	1.7	0.32399
I1	4.17	4.9	10.8	2.9	1.7	0.38	11.4	2.7	1.46	0.48	8.71	3.1	0.28232
I2	6.05	5.9	8.14	2.3	1.31	0.301	13.5	3.2	1.18	0.4	7.72	2.8	0.2796
J1	0.694	1.4	3.94	1.8	0.85	0.21	3.63	0.88	0.726	0.26	2.9	1.6	0.32375
J2	7.82	7.4	19.7	5.1	2.88	0.63	34.5	8	2.43	0.79	11.4	4	0.30924
K1	1.07	1.8	6.98	2	1.49	0.33	10.4	2.5	1.31	0.44	4.65	2.4	0.29416
K2	2.77	3.7	8.05	2.3	1.43	0.32	12.4	2.9	1.19	0.4	6.05	2.9	0.27081
L1	2.21	2.9	5.24	2	1.21	0.28	6.91	1.6	1.03	0.35	5.38	2	0.26361
L2	3.38	2.75	6.1	1.9	1.88	0.47	10.4	2.5	0.947	0.33	6.29	2.8	0.28554

Annexure 2:

M1	2.13	2	5.25	1.6	0.889	0.2	5.43	1.3	0.727	0.26	2.83	1.6	0.26006
M2	1.4	1.3	4.09	1.3	0.915	0.21	9.16	2.2	0.906	0.31	5	1.9	0.25364
N1	6.12	6.1	13.8	3.8	2.04	5	25	5.8	1.16	0.41	7.01	3.2	0.24573
N2	6.41	6.8	4.96	2.2	1.95	0.49	19.2	4.5	1.1	0.38	7.24	2.7	0.23878
O1	2.64	3.4	4.38	2	1.15	0.27	11.5	2.7	0.908	0.32	4.64	2.3	0.31294
O2	8.44	8.2	8.81	3.5	2.27	0.56	18.4	4.3	1.17	0.4	9.28	3.8	0.28295
P1	3.76	4	7.22	2	0.909	0.21	9.14	2.2	0.845	0.29	3.54	1.9	0.2636
P2	3.99	3.9	6.83	1.9	1.06	0.24	10	2.4	0.992	0.34	7.75	3.9	0.2841705
Q1	2.57	3	8.06	2.2	1.28	0.28	10.7	2.5	1.05	0.36	5.23	3.1	0.27661
Q2	3.5	3.5	6.82	1.89	1.32	0.29	11.8	2.7	1.04	0.36	5.58	3.1	0.32846
R1	2.1	2.6	4.02	1.3	1.1	0.25	9.6	2.3	1.04	0.36	5.78	3.1	0.28104
R2	2.4	2.9	4.66	1.5	0.96	0.22	9.4	2.2	0.845	0.3	5.88	2.2	0.28744
S1	2.47	2.6	6.87	2.3	1.45	0.34	8.67	2.1	1.27	0.43	10	3.5	0.30703
S2	2.8	3.4	19.4	4.8	1.63	0.36	9.9	2.3	1.28	0.43	7.86	3.4	0.23429
U1	4.32	5.2	12.3	3.3	2.25	0.54	21.9	5.1	1.45	0.49	7.65	2.8	0.28395
U2	3.19	3.7	8.01	2.3	1.13	0.26	15.3	3.6	1.06	0.36	3.54	1.8	0.26853
W1	6.17	6	50.8	12.1	2.67	0.6	22.1	5.2	1.98	0.65	5.37	2	0.25485
W2	7.83	7.7	12	4.1	2.31	0.58	23.3	5.4	1.15	0.4	5.9	2.7	0.31582
X1	1.97	2.5	5.99	1.8	0.998	0.23	11.2	2.6	0.94	0.33	7.04	2.6	0.3426
X2	2.14	2.7	2.74	1.4	1.05	0.24	10.7	2.5	0.846	0.3	4.51	2.4	0.26497
Y1	2.25	3	9.65	2.7	1.41	0.33	14.3	3.4	1.22	0.41	7.32	3.3	0.28358

b) Table 2 showing corrected results for effieciency and geometry of sample holder

sample name	Pb210 46.5 keV		U238 92.4 keV		Th228 238 keV		Ra226 351 keV		Ra228 911keV		K40 1460.5 keV	
	A (Bq)	E (Bq)	A (Bq)	E (Bq)	A (Bq)	E (Bq)	A (Bq)	E (Bq)	A (Bq)	E (Bq)	A (Bq)	E (Bq)
A1	1.10E+03	1.05E+03	2.10E+02	7.12E+01	5.38E+01	1.29E+01	3.76E+02	8.76E+01	3.17E+01	1.04E+01	1.17E+02	4.26E+01
B1	1.08E+02	2.08E+02	1.14E+02	3.21E+01	2.01E+01	4.47E+00	3.62E+01	8.89E+00	1.72E+01	5.89E+00	9.72E+01	3.54E+01
B2	5.44E+02	7.07E+02	1.49E+02	4.29E+01	2.63E+01	5.84E+00	2.26E+02	5.36E+01	2.27E+01	7.85E+00	1.40E+02	5.11E+01
C1	6.02E+02	6.00E+02	1.15E+02	3.34E+01	2.10E+01	4.75E+00	1.38E+02	3.30E+01	1.49E+01	5.22E+00	9.07E+01	3.15E+01
Cs	2.62E+02	3.66E+02	7.12E+01	2.37E+01	1.10E+01	2.53E+00	1.12E+02	2.68E+01	9.42E+00	3.29E+00	4.03E+01	1.63E+01
D1	5.00E+02	6.08E+02	1.11E+02	3.25E+01	1.90E+01	4.92E+00	1.55E+02	3.72E+01	1.54E+01	5.44E+00	4.29E+01	2.42E+01
E1	4.51E+02	4.51E+02	1.36E+02	3.66E+01	1.99E+01	4.50E+00	1.37E+02	2.57E+01	1.53E+01	5.22E+00	1.39E+02	6.41E+01
F1	4.78E+02	4.78E+02	1.51E+02	4.10E+01	2.33E+01	5.22E+00	2.27E+02	5.36E+01	2.03E+01	6.82E+00	9.75E+01	4.02E+01
Fs	3.05E+02	4.33E+02	3.99E+02	3.37E+01	3.03E+01	7.49E+00	2.05E+02	4.76E+01	1.63E+01	5.58E+00	3.13E+01	2.72E+01
G1	3.04E+02	4.42E+02	9.20E+01	2.79E+01	1.65E+01	3.75E+00	1.43E+02	3.41E+01	1.58E+01	5.38E+00	9.12E+01	4.64E+01
G2	5.73E+02	6.70E+02	1.68E+02	4.50E+01	1.77E+01	4.01E+00	2.01E+02	4.76E+01	1.68E+01	5.70E+00	1.03E+02	3.81E+01
H1	8.34E+02	8.08E+02	1.49E+02	4.07E+01	2.12E+01	4.69E+00	1.93E+02	4.50E+01	1.67E+01	5.66E+00	1.08E+02	8.74E+01
H2	8.67E+02	8.35E+02	1.31E+02	3.57E+01	1.94E+01	4.29E+00	2.09E+02	4.85E+01	1.59E+01	5.46E+00	4.40E+01	2.38E+01
I1	7.68E+02	9.03E+02	1.84E+02	4.95E+01	2.88E+01	6.44E+00	1.92E+02	4.56E+01	2.41E+01	7.91E+00	1.40E+02	4.99E+01
I2	1.13E+03	1.10E+03	1.40E+02	3.96E+01	2.24E+01	5.15E+00	2.30E+02	5.45E+01	1.96E+01	6.66E+00	1.25E+02	4.55E+01
J1	1.11E+02	2.25E+02	5.86E+01	2.68E+01	1.26E+01	3.11E+00	5.34E+01	1.30E+01	1.04E+01	3.74E+00	4.07E+01	2.25E+01
J2	1.31E+03	1.24E+03	3.07E+02	7.94E+01	4.46E+01	9.75E+00	5.32E+02	1.23E+02	3.66E+01	1.19E+01	1.67E+02	5.88E+01
K1	1.89E+02	3.18E+02	1.14E+02	3.27E+01	2.43E+01	5.37E+00	1.68E+02	4.05E+01	2.07E+01	6.96E+00	7.18E+01	3.71E+01
K2	5.32E+02	7.10E+02	1.43E+02	4.09E+01	2.53E+01	5.66E+00	2.18E+02	5.10E+01	2.04E+01	6.87E+00	1.01E+02	4.87E+01
L1	4.36E+02	5.72E+02	9.57E+01	3.65E+01	2.20E+01	5.09E+00	1.25E+02	2.89E+01	1.82E+01	6.18E+00	9.27E+01	3.45E+01
L2	6.16E+02	5.01E+02	1.03E+02	3.21E+01	3.15E+01	7.88E+00	1.74E+02	4.17E+01	1.54E+01	5.38E+00	1.00E+02	4.45E+01

M1	4.26E+02	4.00E+02	9.72E+01	2.96E+01	1.64E+01	3.68E+00	9.95E+01	2.38E+01	1.30E+01	4.65E+00	4.94E+01	2.80E+01
M2	2.87E+02	2.67E+02	7.77E+01	2.47E+01	1.73E+01	3.96E+00	1.72E+02	4.13E+01	1.66E+01	5.69E+00	8.96E+01	3.40E+01
N1	1.30E+03	1.29E+03	2.71E+02	7.45E+01	3.97E+01	9.74E+01	4.85E+02	1.12E+02	2.20E+01	7.76E+00	1.30E+02	5.92E+01
N2	1.40E+03	1.48E+03	1.00E+02	4.44E+01	3.91E+01	9.82E+00	3.83E+02	8.98E+01	2.14E+01	7.41E+00	1.38E+02	5.14E+01
O1	4.39E+02	5.65E+02	6.74E+01	3.08E+01	1.76E+01	4.13E+00	1.75E+02	4.11E+01	1.35E+01	4.76E+00	6.74E+01	3.34E+01
O2	1.55E+03	1.51E+03	1.50E+02	5.96E+01	3.84E+01	9.48E+00	3.10E+02	7.24E+01	1.92E+01	6.58E+00	1.49E+02	6.10E+01
P1	7.42E+02	7.89E+02	1.32E+02	3.65E+01	1.65E+01	3.81E+00	1.65E+02	3.98E+01	1.49E+01	5.12E+00	6.10E+01	3.27E+01
P2	7.30E+02	7.14E+02	1.16E+02	3.22E+01	1.79E+01	4.04E+00	1.68E+02	4.02E+01	1.62E+01	5.57E+00	1.24E+02	6.24E+01
Q1	4.83E+02	5.64E+02	1.40E+02	3.83E+01	2.22E+01	4.85E+00	1.84E+02	4.31E+01	1.77E+01	6.06E+00	8.59E+01	5.09E+01
Q2	5.54E+02	5.54E+02	1.00E+02	2.77E+01	1.92E+01	4.23E+00	1.71E+02	3.92E+01	1.47E+01	5.10E+00	7.72E+01	4.29E+01
R1	3.89E+02	4.81E+02	6.89E+01	2.23E+01	1.87E+01	4.26E+00	1.63E+02	3.90E+01	1.72E+01	5.96E+00	9.34E+01	5.01E+01
R2	4.34E+02	5.25E+02	7.81E+01	2.51E+01	1.60E+01	3.66E+00	1.56E+02	3.65E+01	1.37E+01	4.86E+00	9.29E+01	3.48E+01
S1	4.18E+02	4.40E+02	1.08E+02	3.61E+01	2.26E+01	5.30E+00	1.35E+02	3.26E+01	1.92E+01	6.52E+00	1.48E+02	5.18E+01
S2	6.21E+02	7.55E+02	3.99E+02	9.87E+01	3.33E+01	7.36E+00	2.01E+02	4.68E+01	2.54E+01	8.54E+00	1.52E+02	6.59E+01
U1	7.91E+02	9.52E+02	2.09E+02	5.60E+01	3.79E+01	9.10E+00	3.68E+02	8.56E+01	2.38E+01	8.03E+00	1.22E+02	4.48E+01
U2	6.18E+02	7.16E+02	1.44E+02	4.13E+01	2.01E+01	4.64E+00	2.72E+02	6.39E+01	1.84E+01	6.24E+00	5.99E+01	3.05E+01
W1	1.26E+03	1.22E+03	9.60E+02	2.29E+02	5.02E+01	1.13E+01	4.13E+02	9.72E+01	3.62E+01	1.19E+01	9.57E+01	3.57E+01
W2	1.29E+03	1.27E+03	1.83E+02	6.25E+01	3.50E+01	8.79E+00	3.52E+02	8.15E+01	1.69E+01	5.89E+00	8.49E+01	3.88E+01
X1	2.99E+02	3.79E+02	8.42E+01	2.53E+01	1.39E+01	3.21E+00	1.56E+02	3.62E+01	1.28E+01	4.48E+00	9.34E+01	3.45E+01
X2	4.20E+02	5.30E+02	4.98E+01	2.55E+01	1.90E+01	4.34E+00	1.92E+02	4.50E+01	1.49E+01	5.27E+00	7.73E+01	4.11E+01
Y1	4.13E+02	5.50E+02	1.64E+02	4.59E+01	2.38E+01	5.57E+00	2.40E+02	5.71E+01	2.00E+01	6.73E+00	1.17E+02	5.29E+01

Annexure 3:

The sampling points for the different samples and their GPS points

GPS point	latitude (°)	longitude (°)	altitude (m)	date
Point A	-26,1578	27,8540	1645,0	2013-04-15T08:53:25Z
Point B	-26,1589	27,8554	1706,4	2013-04-15T09:00:59Z
Point C	-26,1610	27,8560	1727,1	2013-04-15T09:09:51Z
Point D	-26,1610	27,8564	1727,0	2013-04-15T09:15:45Z
Point C1	-26,1616	27,8561	1735,4	2013-04-15T09:22:56Z
Point F	-26,1618	27,8559	1737,1	2013-04-15T09:32:38Z
Point G	-26,1619	27,8556	1737,0	2013-04-15T09:40:48Z
Point H	-26,1622	27,8556	1740,2	2013-04-15T09:53:33Z
Point I	-26,1623	27,8552	1738,1	2013-04-15T10:01:00Z
Point J	-26,1620	27,8550	1738,4	2013-04-15T10:09:14Z
Point K	-26,1620	27,8542	1738,9	2013-04-15T10:14:13Z
Point L	-26,1621	27,8537	1736,1	2013-04-15T10:16:50Z
Point M	-26,1626	27,8544	1724,9	2013-04-15T10:47:17Z
Point N	-26,1628	27,8542	1725,1	2013-04-15T10:52:07Z
Point P	-26,1625	27,8550	1726,9	2013-04-15T11:02:52Z
Point O	-26,1625	27,8554	1725,7	2013-04-15T11:07:33Z
Point Q	-26,1624	27,8559	1726,6	2013-04-15T11:12:46Z
Point R	-26,1624	27,8565	1726,1	2013-04-15T11:18:37Z
Point S	-26,1620	27,8564	1725,9	2013-04-15T11:27:25Z
Point T	-26,1626	27,8566	1725,1	2013-04-15T11:32:47Z
Point U	-26,1619	27,8523	1713,1	2013-04-15T11:46:04Z
Point W	-26,1616	27,8531	1712,2	2013-04-15T12:00:51Z
Point X	-26,1622	27,8520	1726,6	2013-04-15T12:15:37Z
Point Z	-26,1573	27,8516	1699,9	2013-04-15T12:28:50Z
Point Z2	-26,1574	27,8519	1691,8	2013-04-15T12:30:58Z

Annexure 4:

Annual uptakes of radionuclides from dust inhalation by different age groups (NNR, 2013)

	Uptake	< 1 a	1 - 2 a	2 -7 a	7 - 12 a	12 - 17 a	> 17 a
^{238}U	S	2.90E-05	2.50E-05	1.60E-05	1.00E-05	8.70E-06	8.00E-06
^{234Th}	S	4.10E-08	3.10E-08	1.70E-08	1.10E-08	9.10E-09	7.70E-09
^{234}U	S	3.30E-05	2.90E-05	1.90E-05	1.20E-05	1.00E-05	9.40E-06
^{230Th}	F	2.10E-04	2.00E-04	1.40E-04	1.10E-04	9.90E-05	1.00E-04
^{226}Ra	S	3.40E-05	2.90E-05	1.90E-05	1.20E-05	1.00E-05	9.50E-06
^{214}Pb	S	6.90E-08	5.00E-08	2.80E-08	2.10E-08	1.50E-08	1.50E-08
^{214}Bi	M	8.70E-08	6.10E-08	3.10E-08	2.20E-08	1.70E-08	1.40E-08
^{210}Pb	S	1.80E-05	1.80E-05	1.10E-05	7.20E-06	5.90E-06	5.10E-06
^{210}Bi	M	3.90E-07	3.00E-07	1.90E-07	1.30E-07	1.10E-07	9.30E-08
^{210}Po	S	1.80E-05	1.40E-05	8.60E-06	5.90E-06	5.10E-06	4.30E-06
^{232}Th	F	2.30E-04	2.20E-04	1.60E-04	1.30E-04	1.20E-04	1.10E-04
^{228}Ra	S	4.90E-05	4.80E-05	3.20E-05	2.00E-05	1.60E-05	1.60E-05
^{228}Ac	F	1.80E-07	1.60E-07	9.70E-08	5.70E-08	2.90E-08	2.50E-08
^{228Th}	$F_{(<7)}, S_{(>7)}$	1.80E-04	1.50E-04	8.30E-05	5.50E-05	4.70E-05	4.00E-05
^{224}Ra	S	1.20E-05	9.20E-06	5.90E-06	4.40E-06	4.20E-06	3.40E-06
^{212}Pb	S	6.70E-07	5.00E-07	3.30E-07	2.50E-07	2.40E-07	.90E-07
^{212}Bi	M	1.60E-07	1.10E-07	6.00E-08	4.40E-08	3.80E-08	3.10E-08

NB: table adapted from NNR regulatory guide 002
S - Slow absorption class
M - Medium absorption class
F - Fast absorption class